Article

Flexible scaling and persistence of social vocal communication

https://doi.org/10.1038/s41586-021-03403-8

Received: 20 March 2020

Accepted: 26 February 2021

Published online: 31 March 2021

Check for updates

Jingyi Chen[1,2], Jeffrey E. Markowitz[3], Varoth Lilascharoen[4], Sandra Taylor[1], Pete Sheurpukdi[1], Jason A. Keller[5], Jennifer R. Jensen[1], Byung Kook Lim[6], Sandeep Robert Datta[3] & Lisa Stowers[1]✉

Innate vocal sounds such as laughing, screaming or crying convey one's feelings to others. In many species, including humans, scaling the amplitude and duration of vocalizations is essential for effective social communication[1–3]. In mice, female scent triggers male mice to emit innate courtship ultrasonic vocalizations (USVs)[4,5]. However, whether mice flexibly scale their vocalizations and how neural circuits are structured to generate flexibility remain largely unknown. Here we identify mouse neurons from the lateral preoptic area (LPOA) that express oestrogen receptor 1 (LPOA^{ESR1} neurons) and, when activated, elicit the complete repertoire of USV syllables emitted during natural courtship. Neural anatomy and functional data reveal a two-step, di-synaptic circuit motif in which primary long-range inhibitory LPOA^{ESR1} neurons relieve a clamp of local periaqueductal grey (PAG) inhibition, enabling excitatory PAG USV-gating neurons to trigger vocalizations. We find that social context shapes a wide range of USV amplitudes and bout durations. This variability is absent when PAG neurons are stimulated directly; PAG-evoked vocalizations are time-locked to neural activity and stereotypically loud. By contrast, increasing the activity of LPOA^{ESR1} neurons scales the amplitude of vocalizations, and delaying the recovery of the inhibition clamp prolongs USV bouts. Thus, the LPOA disinhibition motif contributes to flexible loudness and the duration and persistence of bouts, which are key aspects of effective vocal social communication.

Female odour innately arouses male mice to advertise their desire to mate. Male mice use both chemical and auditory systems to communicate their enthusiasm and location by releasing pheromones through urine scent marking and emitting social sounds (USVs)[5,6]. In the laboratory, USV calling behaviour is robust; most tested male mice produce 40–90-kHz USV calls within 2 min of exposure to female urine odour (Fig. 1a, Supplementary Video 1). Although the neural circuits and mechanisms that regulate vocal learning in birds and humans have been well studied[7,8], how innate sounds are generated and modulated by social context is largely unknown. To identify neural correlates of social sounds, we evaluated the expression of the c-FOS transcription factor as a proxy of neural activity from male mice that generated odour-evoked USVs. We focused on the hypothalamus—a region known to promote social and sexual behaviours including ultrasonic vocalizations[9–11]—and found an increase in c-FOS expression in a band from the caudal bed nucleus of the stria terminalis to the LPOA, and into the medial preoptic area (Extended Data Fig. 1a).

Hypothalamus promotes social USVs

Neurons in the hypothalamus are molecularly and functionally heterogeneous[12,13]. We used a candidate marker approach to identify a subset of neurons that elicit social calls. We found that 80% of c-FOS^{+} cells overlapped with LPOA neurons that express oestrogen receptor 1 (LPOA^{ESR1}) (Fig. 1b, Extended Data Fig. 1b–d). We investigated the in vivo temporal correlation between neural activity and USV sounds during natural social behaviour using a reporter of calcium influx, GCaMP6s, expressed in the LPOA of knock-in mice that express Cre recombinase under control of the *Esr1* promoter (LPOA$^{ESR1/GCaMP6s}$ mice). Indeed, socially evoked USVs correlated with an increase in LPOA$^{ESR1/GCaMP6s}$ fluorescence measured by fibre photometry (Extended Data Fig. 2a–f). To study whether the LPOA^{ESR1} neurons mediate natural male courtship vocalizations, we restricted the expression of the DREADD receptors hM_4D_i specifically to the LPOA^{ESR1} neurons and performed clozapine-*N*-oxide (CNO)-meditated inhibition in the presence of an awake, freely behaving female mouse to evoke social behaviour in the male mouse (Fig. 1c, d). All CNO-injected LPOA$^{ESR1/hM4Di}$ male mice emitted fewer USVs, consistent with the participation of an ESR1-expressing subset of LPOA neurons in promoting USV production (Fig. 1c, d, Extended Data Fig. 2g–o). CNO inhibition of LPOA$^{ESR1/hM4Di}$ neurons did not alter other features of male courtship or sensation of the female, such as sniffing and mounting behaviours (Extended Data Fig. 2l).

We also investigated the sufficiency of the LPOA^{ESR1+} neuron subset in USV production by expressing channelrhodopsin (ChR2) in the LPOA of

[1]Department of Neuroscience, Scripps Research, La Jolla, CA, USA. [2]Biomedical Sciences Graduate Program, Scripps Research, La Jolla, CA, USA. [3]Department of Neurobiology, Harvard Medical School, Boston, MA, USA. [4]Biological Sciences Graduate Program, University of California San Diego, La Jolla, CA, USA. [5]Janelia Research Campus, Howard Hughes Medical Institute, Ashburn, VA, USA. [6]Neurobiology Section, Division of Biological Sciences, University of California San Diego, La Jolla, CA, USA. ✉e-mail: stowers@scripps.edu

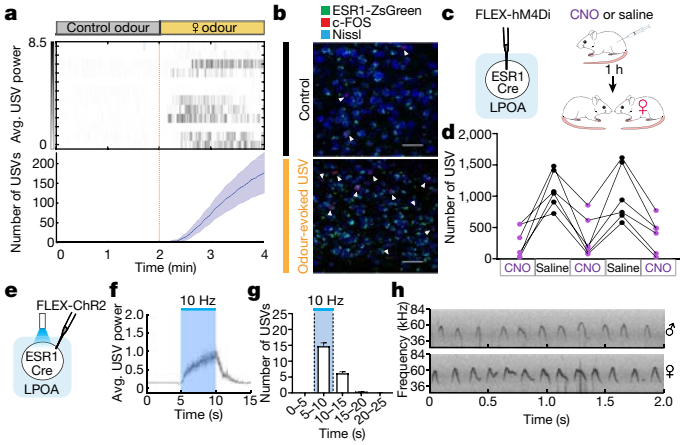

Fig. 1 | Hypothalamic LPOA^{ESR1} neurons underlie USV social calling. a, Raster plot (top) and mean number (bottom) of USVs emitted by naive male mice during interaction with tonic water control odour (grey) or with female mouse urine odour (yellow). Data are mean ± s.e.m. $n = 12$ mice. **b**, Expression of c-FOS and ESR1 in the LPOA of a male mouse after interaction with control odour (black) or female mouse odour (yellow). Scale bars, 50 µm. **c**, Experimental design for the LPOA^{ESR1} chemoinhibition experiment. **d**, Number of USVs in the presence of behaving female mice after male mice received injections of either CNO or saline on alternative days over 5 test days. $n = 6$ mice. **e**–**h**, LPOA$^{ESR1/ChR2}$ neurons evoke USVs. **e**, ChR2 virus injection in the LPOA region of ESR1-Cre mice. **f**, Average USV power evoked by photostimulation of LPOA$^{ESR1/ChR2}$ neurons at 10 Hz (5-s duration, 15-ms pulses). Solid line indicates the mean of all trials; shaded region indicates 95% confidence interval. **g**, Number of USVs detected during photostimulation of LPOA^{ESR1+} cells. Data are mean ± s.e.m. (both sexes, $n = 34$ mice). **h**, Sample USV sonograms evoked during photostimulation of male or female mice.

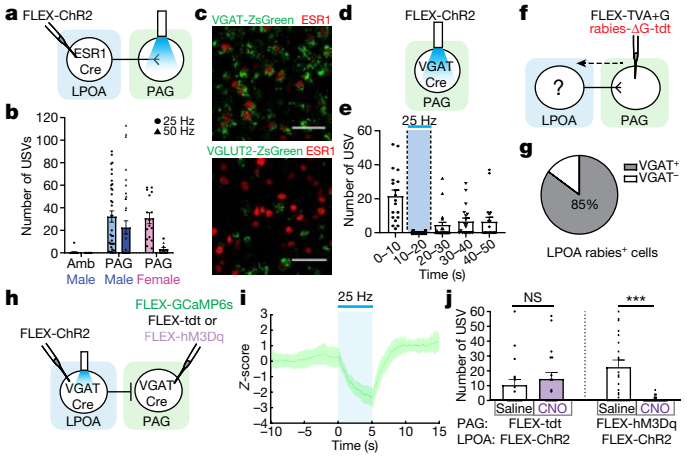

Fig. 2 | LPOA^{VGAT}–PAG^{VGAT}–PAG^{VGLUT2} di-synaptic disinhibition circuit triggers USVs. a, **b**, LPOA$^{ESR1/ChR2}$ axon terminal photostimulation in the PAG evokes USV calls. **a**, Experimental design. **b**, Number of USVs detected in the nucleus ambiguous (Amb) ($n = 5$ male mice) and the PAG ($n = 13$ and 4 male and female mice, respectively). Data are mean ± s.e.m. **c**, Sample images of the co-expression of ESR1 and VGAT-ZsGreen (top, $n = 4$ mice, 3 sections per mouse) and VGLUT2-ZsGreen (bottom, $n = 3$ mice, 3 sections per mouse) in LPOA^{ESR1+} neurons. Scale bars, 50 µm. **d**, **e**, Photostimulation (blue bar) of male inhibitory PAG$^{VGAT/ChR2}$ neurons during social interaction with an awake female mouse blocks natural USVs. **d**, Experimental design to express ChR2 in local inhibitory PAG neurons. **e**, Quantification of evoked USV syllables. Data are mean ± s.e.m. $n = 3$ mice, 19 trials. **f**, Experimental design to assess direct anatomy to LPOA by retrograde tracing from PAG^{VGAT} cells. tdt, tdTomato. **g**, Percentage of rabies-tdTomato expression in LPOA VGAT^{+} cells. $n = 3$ mice, 320 cells counted. **h**, Experimental design to express ChR2 in LPOA^{VGAT} neurons, and GCaMP6s, tdTomato or hM$_3$D$_q$ in PAG^{VGAT} neurons. **i**, Mean z-score of fibre photometry signal from PAG$^{VGAT/GCaMP6s}$ neurons after 25 Hz photostimulation (blue bar) on LPOA$^{VGAT/ChR2}$ cells. Solid line indicates mean of all trials; shaded region indicates 95% confidence interval. $n = 4$ mice, 4 trials per mouse. **j**, USVs are silenced during photostimulation of LPOA$^{VGAT/ChR2}$ after CNO treatment on PAG$^{VGAT/hM3Dq}$ neurons. Data are mean ± s.e.m. $n = 3$ mice, 36 trials (hM$_3$D$_q$), 18 trials (tdt control). ***$P = 0.005$, paired Wilcoxon test, two sided. NS, not significant ($P > 0.05$).

ESR1-Cre mice (LPOA$^{ESR1/ChR2}$). Photostimulation activated LPOA$^{ESR1/ChR2}$ neurons (Fig. 1e, Extended Data Fig. 3a, b) and evoked USV calling in both male and female mice in the absence of any sensory stimulation[14] (Fig. 1f–h, Extended Data Fig. 3c–g, Supplementary Video 2). To investigate the repertoire of male photoactivated USVs, we used an automated and unsupervised signal processing approach (MUPET[15]) to evaluate their composition compared to natural calls produced by male mice in response to a variety of social stimuli as well as infant pup calls. Photostimulation of LPOA$^{ESR1/ChR2}$ neurons did not simply produce repetitive stuttering of USV syllables. Instead, it evoked a rich repertoire of both simple and complex USV syllables, such as those displayed during natural social interactions (Extended Data Fig. 4). These findings indicate that LPOA^{ESR1} neurons can trigger a suite of USV syllables that match a natural range of USVs and provide a cellular handle to study the circuits and mechanisms that underlie the generation of innate social sounds.

USV production in mice is known to depend on neurons in the PAG that gate the activity of motor neurons in the nucleus ambiguus (Amb)[16,17]. We performed anatomical tracing and functional manipulation to determine whether the LPOA^{ESR1} neurons promote USV calling through either of these known nodes (Extended Data Fig. 5a–f). Directly stimulating the sparse terminals in the nucleus ambiguous failed to elicit USVs, but photoactivation of LPOA^{ESR1} neurons to the PAG terminals triggered robust USV calling in both male and female mice, similar to that observed from LPOA^{ESR1} soma stimulation (Fig. 2a, b, Extended Data Fig. 5g–m). These data demonstrate that LPOA^{ESR1} neurons provide an anatomical and functional route that link social behaviour-promoting centres to the established PAG-gating neurons to trigger vocalizations.

Disinhibition motif triggers USV calling

PAG USV-gating neurons are known to be excitatory (PAG^{VGLUT2})[17] and we observed that activation of LPOA^{ESR1} neurons produces USV calling (Fig. 1e–h). Therefore, feedforward excitation would be the simplest circuit arrangement through which LPOA^{ESR1} neurons could drive vocalizations. Instead, multiplex fluorescent in situ hybridization and immunohistochemistry of ESR1 in knock-in VGAT-Ai6 ($n = 3$, 10,340 cells quantified) or VGLUT2-Ai6 mice ($n = 4$, 11,082 cells quantified) revealed that the ratio of LPOA$^{ESR1/VGAT}$ to LPOA$^{ESR1/VGLUT2}$ neurons is five to one (Fig. 2c, Extended Data Fig. 6a–c). Ex vivo cell-attached recordings of lateral PAG cells during photostimulation of LPOA$^{ESR1/ChR2}$ terminals confirmed that some LPOA$^{ESR1/ChR2}$ neurons are functionally inhibitory. Whole-cell voltage-clamp recordings of the PAG cells revealed inhibitory action on PAG cells from photostimulated LPOA$^{ESR1/ChR2}$ neurons, with inhibitory postsynaptic currents (IPSCs) locked with light pulses consistent with a monosynaptic arrangement (Extended Data Fig. 6d–g). To compare the functional relevance of both the LPOA excitatory and inhibitory PAG projections, we expressed ChR2 in the LPOA of knock-in mice expressing Cre under the control of either VGAT or VGLUT2 (LPOA$^{VGAT/ChR2}$ or LPOA$^{VGLUT2/ChR2}$, respectively). Photoactivation of LPOA$^{VGLUT2/ChR2}$ neurons did not produce any vocal sounds (Extended Data Fig. 6h–j). By contrast, photostimulation of LPOA$^{VGAT/ChR2}$ neurons was sufficient to elicit USV calling (Extended Data Fig. 6k, l). Together, these results identify the subset of LPOA^{ESR1} neurons that facilitate USV social calling as long-range inhibitory neurons.

Instead of eliciting USV calling through direct feedforward excitation, these long-range inhibitory LPOA^{ESR1} neurons may trigger behaviour by relieving the PAG USV-gating neurons from local inhibition. In addition to excitatory USV-gating neurons in the lateral PAG[17], there

are clusters of local inhibitory neurons in the ventral lateral PAG[18,19] (PAG^{VGAT}) (Extended Data Fig. 6m). Circuit tracing and functional ex vivo recordings were consistent with monosynaptic inhibitory connections between the local PAG^{VGAT} neurons and the PAG^{VGLUT2} USV-gating cells (Extended Data Fig. 7a–h). Before photostimulation, $PAG^{VGAT/ChR2}$ male mice naturally initiated USV calling while freely behaving with female mice; however, driving the local inhibitory activity with light stimulation of $PAG^{VGAT/ChR2}$ neurons at 1 or 5 Hz reduced the number of socially evoked USV calls, and stimulation at 10 Hz (or higher) immediately halted USV emission evoked by female odour (Fig. 2d, e, Extended Data Fig. 7i, j). These experiments indicate that the PAG USV-gating neurons are under a direct clamp of local inhibition produced by PAG^{VGAT} neurons.

We next investigated whether the $LPOA^{ESR1}$ cells trigger calling by relieving this local PAG inhibition. Conditional retrograde tracing from the local PAG inhibitory neurons (PAG^{VGAT}) and multiplex fluorescent in situ hybridization (Fig. 2f, g, Extended Data Fig. 8a–c) confirmed the anatomy of the circuit while ex vivo whole-cell recording of PAG^{VGAT} cells after light stimulation of $LPOA^{VGAT/ChR2}$ terminals and photostimulation of the LPOA with fibre-photometry in the PAG of VGAT-Cre mice functionally supported this inhibition circuit ($LPOA^{VGAT/ChR2}$; $PAG^{VGAT/GCaMP6s}$) (Fig. 2h, i, Extended Data Fig. 8d–h). To further validate whether the flow of information is consistent with LPOA-driven disinhibition, we designed an experimental model in VGAT-Cre mice that combines optogenetic activation of the LPOA (to trigger USVs) while artificially strengthening the local PAG inhibitory signals with chemogenetic activation ($PAG^{VGAT/hM3Dq}$) (Fig. 2h). CNO-mediated activation of $PAG^{VGAT/hM3Dq}$ neurons completely blocked LPOA-photostimulated USV calls even with $LPOA^{VGAT/ChR2}$ stimulation as high as 50 Hz (Fig. 2j). Thus, activating the inhibitory $LPOA^{ESR1}$ neurons inhibits the clamp of local inhibition from the PAG^{VGAT} cells, which enables excitatory activity of the nucleus ambiguous-projecting USV-gating PAG neurons to trigger USVs[11,19].

Context scales natural USVs

Circuits that underlie complex innate behaviours such as parenting and fear also include a two-step di-synaptic disinhibition motif to activate the PAG, but how this motif contributes to behavioural actions remain unknown[18,19]. Our simple behaviour enables us to study how circuit and cellular properties of the LPOA and PAG contribute to features of USV production. Mouse USVs are often analysed for the identity and arrangement of syllables as these are crucial features in learned human language and birdsong[4,7,8,16,20,21]. Although the type of syllable is critical for language, innate social sounds are effective because they scale a simple noise from soft and few to loud and many (a giggle compared to hearty laughter)[2,22]. Such vocal flexibility effectively transmits one's internal state to others[1–3]. Whether the amplitude and duration of mouse USVs are fixed or can flexibly scale during social and sensory-evoked behaviour remains largely unstudied[23]. We developed improved automated methods to reliably detect USV sounds during noisy natural behaviour (Extended Data Fig. 9a) and used this approach to measure USVs from male mice freely behaving with a variety of relevant social stimuli[22].

The sensation of behaving female mice or female odour reliably evokes male mice to produce abundant, short-latency, low inter-syllable interval USV syllables, whereas male mice or male odour evoked fewer USVs that were produced unreliably[5,23–25] (Fig. 3a, Extended Data Fig. 8i–k). We next analysed syllable organization. Syllables are minimally separated by a single breath[4,23,26], grouped in phrases or strings of syllables called bouts (Fig. 1h, Extended Data Fig. 9b). We observed bout length flexibly adapted to social context. Awake female mice and female odour sensation promoted male mice to generate longer USV bouts (averaging 7–10 s) that were on average 50% louder than shorter USV bouts (averaging 1–2 s) evoked by anaesthetized female mice and male mouse cues (Fig. 3b–d). Within a social context, bout length also varied dynamically. Male mice emitted USV bouts as short as several syllables and as long as 17 s in the presence of awake behaving female mice, and USV loudness in single USV bouts were produced over a fivefold range in amplitude (Fig. 3b–d). Overall, mouse USV syllable numbers, amplitude and bout duration are naturally plastic, scalable and flexibly displayed depending on the identity of the environment or the reliability of social context.

LPOA expands range of USV scaling

To investigate whether the ability to scale USV amplitude and bout duration arises in the identified circuit, we varied the frequency of photostimulation in $PAG^{VGLUT2/ChR2}$ or $LPOA^{ESR1/ChR2}$ neurons from male mice in the absence of female odour, quantified the number of USV syllables, and compared these artificially evoked USVs to natural male calls evoked by social stimuli. Increasing the frequency or the duration of photostimulation of $LPOA^{ESR1/ChR2}$ neurons scaled syllable production from unreliably few and quiet (5 Hz) to robust and loud (50 Hz) (Figs. 3e, h, 4a, c, Extended Data Figs. 9c, d). Notably, even with increasing frequency of stimulation, the structure of distinct syllables remained intact without distortion (Extended Data Fig. 9d, e). Low-frequency photostimulation (5 Hz) of $PAG^{VGLUT2/ChR2}$ neurons produced reliable, robust USVs of relatively high amplitude and fixed bout duration (Figs. 3f, g, i–k, 4b, c). Low-frequency photostimulation (5 Hz) of the $PAG^{VGLUT2/ChR2}$ neurons generated USV bouts that were fourfold longer and twofold louder than those observed from the LPOA stimulated at 5 Hz (Fig. 3j–l). The PAG and the LPOA contribute different features to USV behaviour. $PAG^{VGLUT2/ChR2}$ neurons are less flexible, and display a steep, low threshold that produces many loud syllables and long bouts, whereas the $LPOA^{ESR1/ChR2}$ neurons respond with a gradual, higher threshold that can flexibly reduce the amplitude and bout length (Fig. 3j–l). Together, we found that the PAG USV-gating neurons are poised to generate exuberant USV calls and the di-synaptic inhibition flexibly expands the dynamic range of bout length and amplitude.

Circuit motif enables persistent USVs

Another feature of effective social vocal sounds is the ability to persist beyond immediate sensory initiation. For example, a poor joke may evoke a brief giggle, whereas a clever one evokes laughter that lasts beyond the punchline. We observed that $LPOA^{ESR1/ChR2}$ neurons produced calls that persist beyond the end of photostimulation (Fig. 1f, g). Low-frequency (5 Hz) photostimulation of $LPOA^{ESR1/ChR2}$ neurons produced calls that were largely locked to the presence of light, whereas increasing the frequency of photostimulation increased the persistence of emitted USVs many seconds beyond the termination of light (Fig. 4a, c). By contrast, USV-calling mediated by the activation of the $PAG^{VGLUT2/ChR2}$ USV-gating cells reliably produced USVs tightly locked to the onset and termination of photostimulation (Figs. 3f, 4b, c). USVs evoked by the PAG (and downstream nodes) tightly mirrors incoming circuit activity, whereas the LPOA-to-PAG disinhibition nodes flexibly extends bout duration beyond LPOA activation.

To further investigate the effect of local PAG^{VGAT} cells on USV persistence, we used chemogenetics to release the inhibitory clamp on the PAG USV-gating neurons while stimulating USV calls from the LPOA through optogenetics (Fig. 4d, Extended Data Fig. 10c, e). Silencing the local $PAG^{VGAT/hM4Di}$ neurons lowered the $LPOA^{VGAT/ChR2}$ photostimulation threshold of USV calling to as low as 1 Hz (Extended Data Fig. 10a–f, Supplementary Video 3). Moreover, high-frequency (25 Hz) stimulation of $LPOA^{VGAT/ChR2}$ neurons in the presence of CNO produced extreme prolonged calling that lasted up to 35 s beyond cessation of the photostimulation (Fig. 4e, f, Supplementary Video 3). This prolonged calling effect, which increased syllable number and bout length, scaled across the stimulation frequency range (1–25 Hz) (Extended Data Fig. 10d, f, g). Cell-attached recordings in a slice preparation from labelled PAG^{VGAT}

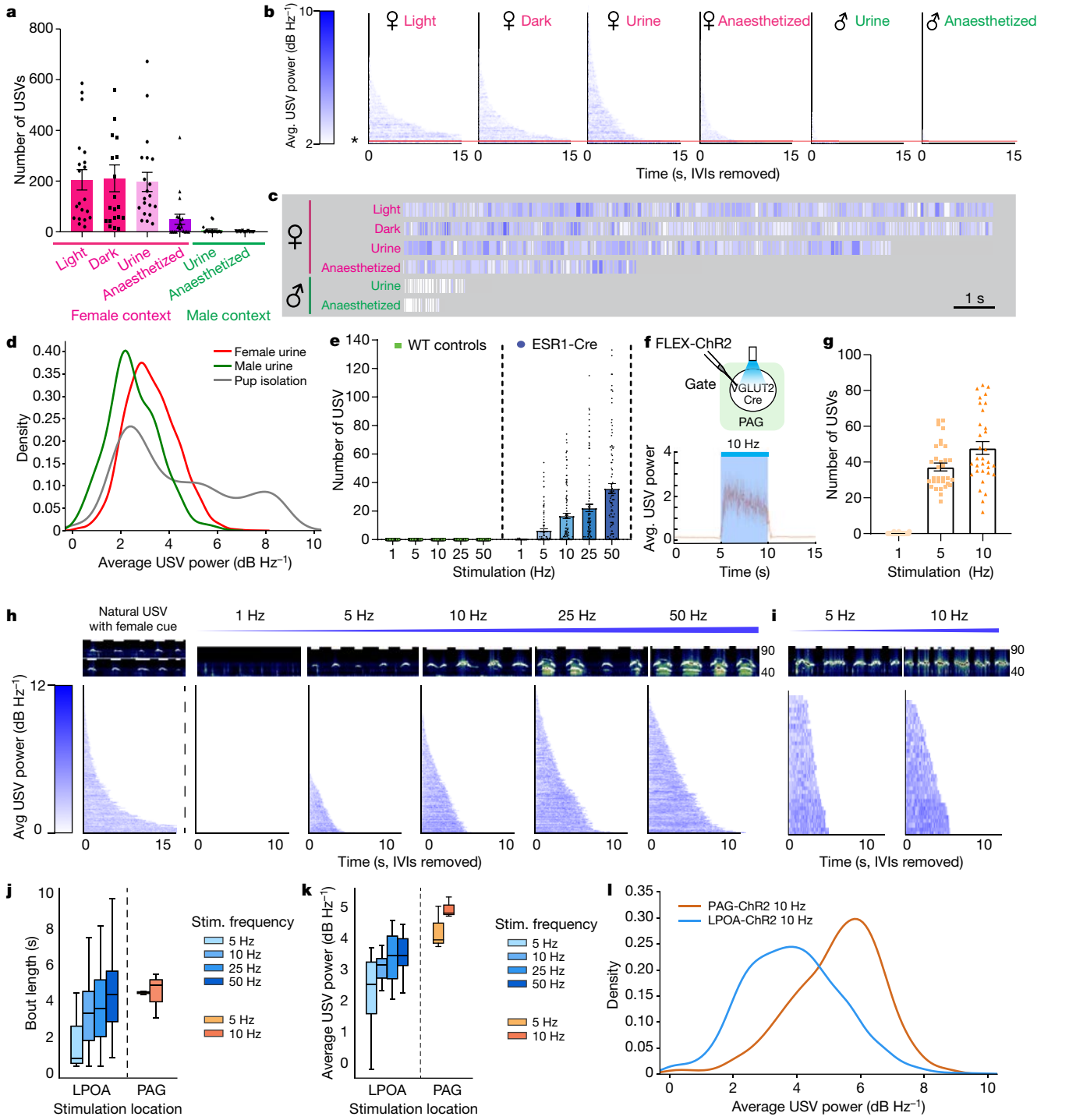

Fig. 3 | LPOA^{ESR1} neuron activity scales USV amplitude and bout duration. **a**–**c**, Wild-type male mice flexibly adjust USV syllable number, amplitude and bout length within and across sensory or social contexts. **a**, Number of USVs produced by male mice during sensory or social interaction. **b**, Raster plot of USV bout length (strings of syllables separated by more than 2-s pauses) emitted by wild-type male mice in different sensory or social contexts sorted by bout length. IVI, inter vocalization intervals. **c**, High-resolution plot of single USV bouts (asterisk and orange line in **b**) showing variable bout length and amplitude (heat map in **b**) emitted by wild-type male mice during sensory or social interaction. Red denotes female mouse sensation; green denotes male mouse sensation. Data are mean ± s.e.m. $n = 20$ mice. **d**, Distribution of average USV power produced by male mice exposed to either male or female urine, and by pups isolated from the nest. **e**, Increasing frequency of photostimulation of LPOA$^{ESR1/ChR2}$ neurons scales the number of USV syllables. Data are mean ± s.e.m. $n = 5$ for wild-type (WT) control, $n = 23$ for ChR2. **f**, Top, experimental design to express ChR2 in the PAG of VGLUT2-Cre knock-in mice. Bottom, average USV power during photostimulation of PAG$^{VGLUT2/ChR2}$ neurons. **g**, Number of USV syllables emitted during photostimulation of PAG$^{VGLUT2/ChR2}$ neurons. Data are mean ± s.e.m. $n = 3$ mice, 32 trials. **h**, Representative sonograms (top) and raster plots (bottom) of USV amplitude and bout lengths emitted by LPOA$^{ESR1/ChR2}$ male mice interacting with female mouse odour or live female mice to evoke natural USVs (left), and in the absence of female mouse with increasing frequency of 5-s light stimulation (right). $n = 26$ mice, sorted by bout length. Sonograms occur in the range of 40–90 kHz. **i**, Representative sonograms (top) and raster plots (bottom) of USV amplitude and bout lengths emitted during 5-s photostimulation of PAG$^{VGLUT2/ChR2}$ neurons at 5 or 10 Hz. $n = 3$ mice. **j**, **k**, Average USV bout length (**j**) and average amplitude of USV (**k**) during photostimulation of either LPOA$^{ESR1/ChR2}$ neurons ($n = 26$ mice) or PAG$^{VGLUT2/ChR2}$ neurons ($n = 3$ mice). Box plots show minimum and maximum values and quantile (0.25, 0.75). **l**, Distribution of mean USV power during 10-Hz photostimulation in either PAG$^{VGLUT2/ChR2}$ or LPOA$^{ESR1/ChR2}$ neurons.

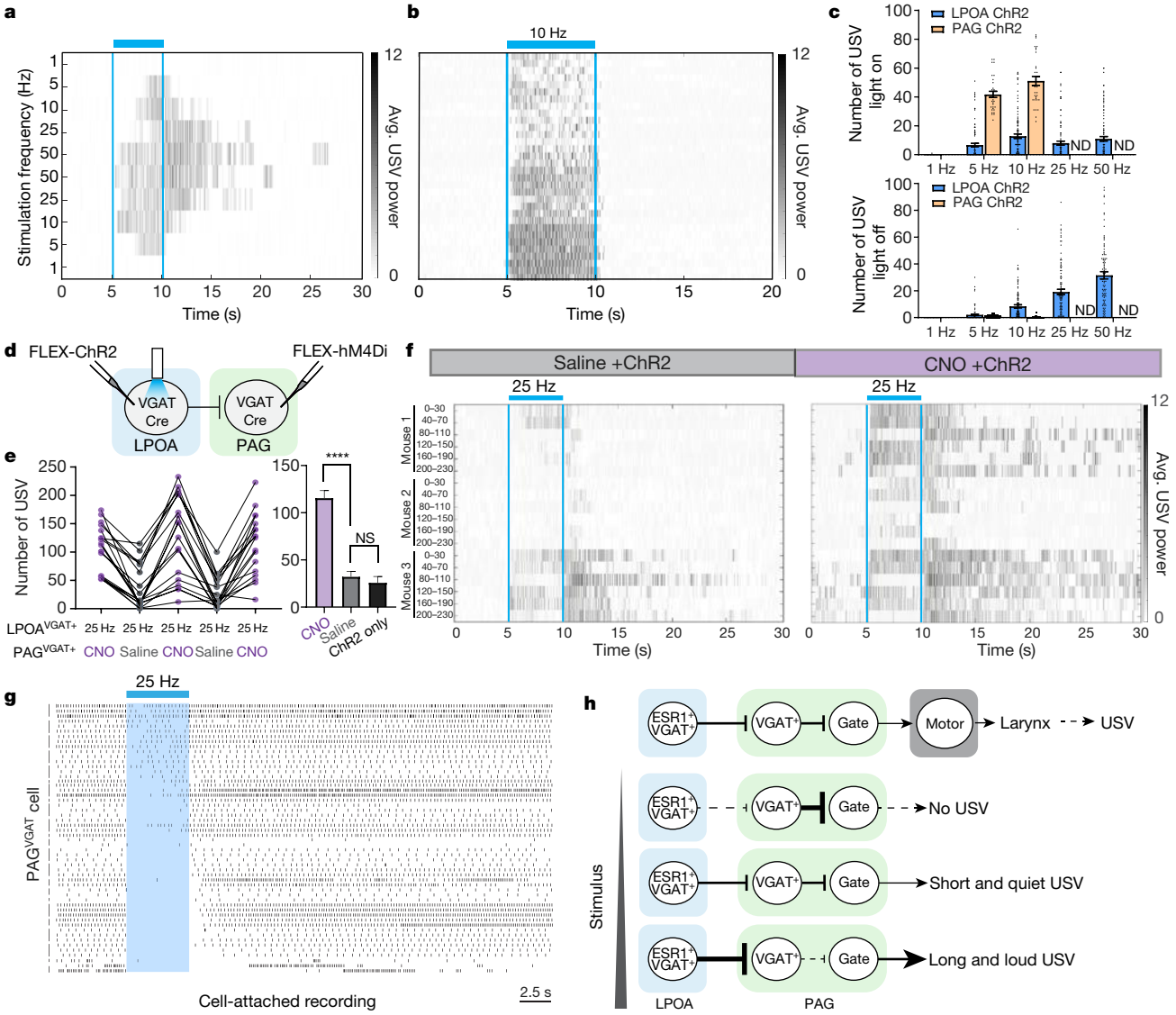

Fig. 4 | Vocal persistence is generated through activity of local PAG^{VGAT} neurons. a, Representative USVs emitted during scaling (ascending and descending frequency) of photostimulation in LPOA$^{ESR1/ChR2}$ neurons from male mice demonstrate that USVs persist after photostimulation ceases (blue bar). **b**, Raster plot of USV syllables emitted during photostimulation of PAG$^{VGLUT2/ChR2}$ neurons at 10 Hz. USVs are locked to light stimulus (blue bars). Each row is a single trial. $n = 3$ mice, 32 trials total. **c**, Number of syllables after photostimulation of either LPOA$^{ESR1/ChR2}$ (blue, $n = 26$ mice, 102 trials) or PAG$^{VGLUT2/ChR2}$ (orange, $n = 3$ mice, 32 trials) neurons during light on (top) or light off (bottom). ND, not determined. **d**, Experimental design to simultaneously express ChR2 in LPOA^{VGAT} neurons and hM$_4$D$_i$ in PAG^{VGAT} cells. **e**, **f**, USVs emitted during photostimulation of LPOA$^{VGAT/ChR2}$ cells after injection of saline as control (grey) or CNO (purple) to inhibit PAG$^{VGAT/hM4Di}$ neurons on alternative days. **e**, USV number during stimulation of LPOA^{VGAT} neurons at 25 Hz. ****$P < 0.0001$, paired Wilcoxon test, two-sided. NS, not significant ($P > 0.05$). **f**, Raster plot of USVs emitted during and after photostimulation (blue bars). Each row is 30 s of a 230-s trial aligned to light stimuli applied every 40 s. Data are mean ± s.e.m. $n = 3$, 6 trials per mouse per test day. **g**, Ex vivo cell-attached recording of PAG^{VGAT} neurons during photostimulating (blue shading) of LPOA$^{VGAT/ChR2}$ axon terminals. $n = 4$ mice, total 23 cells. Left bars group the same cell during several trials. **h**, Model of disinhibition circuitry for USV calling. LPOA disinhibition to scale USV power and bout duration enables flexible responses to social or sensory context.

neurons during photostimulation of LPOA$^{VGAT/ChR2}$ neurons immediately inhibited the spontaneous firing of most PAG^{VGAT} neurons; however, the recovery of spiking was quite variable and asynchronous[27–29] (Fig. 4g). In some cells, this delay to recover inhibitory tone persisted for seconds after photostimulation ended (Fig. 4g) and provides a potential cellular mechanism to support the persistent USV calling behaviour that continues after the offset of LPOA photostimulation in vivo (Fig. 4a, f). Such a feature would be useful for a male mouse to maintain vocal communication of his desire to mate beyond his immediate sensation of a female mouse, such as when she leaves his view, or he loses her odour trail.

The di-synaptic disinhibition between the LPOA and PAG does not simply act as a relay switch that transmits sensory information to motor centres. Instead, we find the PAG USV-gating neurons are kept inactive under a clamp of local PAG inhibition while poised at low threshold to drive robust USV calling. The escalating activity of LPOA^{ESR1} neurons induces disinhibition that enables scaling of USV amplitude from quiet to loud, with the intrinsic extended recovery of the PAG^{VGAT} neuron inhibition prolonging USV bouts (Fig. 4h). These circuit-level features enable vocalizations to persist and calling to continue beyond direct initiation by sensory stimulation. The addition of this LPOA node and disinhibition motif upstream of the PAG USV-gating neuron circuit provides a biological solution for generating the flexible vocal loudness, bout duration, and persistence—all of which are crucial features to effectively communicate the sender's level of affect and arousal to the listener.

Online content

Any methods, additional references, Nature Research reporting summaries, source data, extended data, supplementary information, acknowledgements, peer review information; details of author contributions and competing interests; and statements of data and code availability are available at https://doi.org/10.1038/s41586-021-03403-8.

1. Bachorowski, J. A. & Owren, M. J. Not all laughs are alike: voiced but not unvoiced laughter readily elicits positive affect. *Psychol. Sci.* **12**, 252–257 (2001).
2. Darwin, C. & Prodger, P. *The Expression of the Emotions in Man and Animals* 3rd edn (Harper Collins, 1998).
3. Esposito, G., Nakazawa, J., Venuti, P. & Bornstein, M. H. Judgment of infant cry: the roles of acoustic characteristics and sociodemographic characteristics. *Jpn. Psychol. Res.* **57**, 126–134 (2015).
4. Holy, T. E. & Guo, Z. Ultrasonic songs of male mice. *PLoS Biol.* **3**, e386 (2005).
5. Whitney, G., Alpern, M., Dizinno, G. & Horowitz, G. Female odors evoke ultrasounds from male mice. *Anim. Learn. Behav.* **2**, 13–18 (1974).
6. Keller, J. A. et al. Voluntary urination control by brainstem neurons that relax the urethral sphincter. *Nat. Neurosci.* **21**, 1229–1238 (2018).
7. Brainard, M. S. & Doupe, A. J. Translating birdsong: songbirds as a model for basic and applied medical research. *Annu. Rev. Neurosci.* **36**, 489–517 (2013).
8. Jarvis, E. D. Evolution of vocal learning and spoken language. *Science* **366**, 50–54 (2019).
9. Gao, S. C., Wei, Y. C., Wang, S. R. & Xu, X. H. Medial Preoptic Area Modulates Courtship Ultrasonic Vocalization in Adult Male Mice. *Neurosci. Bull.* **35**, 697–708 (2019).
10. Karigo, T. et al. Distinct hypothalamic control of same- and opposite-sex mounting behaviour in mice. *Nature* **589**, 258–263 (2020).
11. Michael, V. et al. Circuit and synaptic organization of forebrain-to-midbrain pathways that promote and suppress vocalization. *eLife* **9**, e63493 (2020).
12. Fang, Y. Y., Yamaguchi, T., Song, S. C., Tritsch, N. X. & Lin, D. A hypothalamic midbrain pathway essential for driving maternal behaviors. *Neuron* **98**, 192–207.e110 (2018).
13. Moffitt, J. R. et al. Molecular, spatial, and functional single-cell profiling of the hypothalamic preoptic region. *Science* **362**, eaau5324 (2018).
14. Maggio, J. C. & Whitney, G. Ultrasonic vocalizing by adult female mice (*Mus musculus*). *J. Comp. Psychol.* **99**, 420–436 (1985).
15. Van Segbroeck, M., Knoll, A. T., Levitt, P. & Narayanan, S. MUPET-Mouse Ultrasonic Profile ExTraction: A signal processing tool for rapid and unsupervised analysis of ultrasonic vocalizations. *Neuron* **94**, 465–485.e465, (2017).
16. Arriaga, G., Zhou, E. P. & Jarvis, E. D. Of mice, birds, and men: the mouse ultrasonic song system has some features similar to humans and song-learning birds. *PLoS ONE* **7**, e46610 (2012).
17. Tschida, K. et al. A specialized neural circuit gates social vocalizations in the mouse. *Neuron* **103**, 459–472.e454 (2019).
18. Kohl, J. et al. Functional circuit architecture underlying parental behaviour. *Nature* **556**, 326–331 (2018).
19. Tovote, P. et al. Midbrain circuits for defensive behaviour. *Nature* **534**, 206–212 (2016).
20. Doupe, A. J. & Kuhl, P. K. Birdsong and human speech: common themes and mechanisms. *Annu. Rev. Neurosci.* **22**, 567–631 (1999).
21. Sainburg, T., Theilman, B., Thielk, M. & Gentner, T. Q. Parallels in the sequential organization of birdsong and human speech. *Nat. Commun.* **10**, 3636 (2019).
22. Chabout, J., Sarkar, A., Dunson, D. B. & Jarvis, E. D. Male mice song syntax depends on social contexts and influences female preferences. *Front. Behav. Neurosci.* **9**, 76 (2015).
23. Castellucci, G. A., Calbick, D. & McCormick, D. The temporal organization of mouse ultrasonic vocalizations. *PLoS ONE* **13**, e0199929 (2018).
24. Guo, Z. & Holy, T. E. Sex selectivity of mouse ultrasonic songs. *Chem. Senses* **32**, 463–473 (2007).
25. Nyby, J., Wysocki, C. J., Whitney, G., Dizinno, G. & Schneider, J. Elicitation of male mouse ultrasonic vocalizations: I. Urinary cues. *J. Comp. Physiol. Psychol.* **93**, 957–975 (1979).
26. Sirotin, Y. B., Costa, M. E. & Laplagne, D. A. Rodent ultrasonic vocalizations are bound to active sniffing behavior. *Front. Behav. Neurosci.* **8**, 399 (2014).
27. Hefft, S. & Jonas, P. Asynchronous GABA release generates long-lasting inhibition at a hippocampal interneuron-principal neuron synapse. *Nat. Neurosci.* **8**, 1319–1328 (2005).
28. Atasoy, D., Betley, J. N., Su, H. H. & Sternson, S. M. Deconstruction of a neural circuit for hunger. *Nature* **488**, 172–177 (2012).
29. Letzkus, J. J., Wolff, S. B. & Lüthi, A. Disinhibition, a circuit mechanism for associative learning and memory. *Neuron* **88**, 264–276 (2015).

Methods

Data reporting

No statistical methods were used to predetermine sample size. The experiments were not randomized and investigators were not blinded to allocation during experiments and outcome assessment.

Animals

All animal procedures were conducted in accordance with institutional guidelines and protocols approved by the Institutional Animal Care and Use Committee at Scripps Research. BALB/cByJ male mice were group housed at weaning, single housed at 8 weeks old for at least one week before any testing and maintained on a 12 h/12 h light/dark cycle with food and water available ad libitum in a controlled environment (median temperature 21 °C, humidity 50%). For functional manipulation, female and male mice from mouse lines were purchased from The Jackson Laboratory: ESR1-Cre (stock 017911), VGAT-Cre (stock 016962), VGLUT2-Cre (stock 016963), and ROSA-LSL-ZsGreen (Ai6, stock 007906). All mice were backcrossed into the BALB/cByJ background for more than five generations except for the ROSA-LSL-ZsGreen line. Surgeries were performed between 2 and 6 months old and mice were given 2–3 weeks for recovery before behavioural testing that last for 2–5 weeks.

USV recording: adult male mouse USV response to female urine

Adult BALB/cByJ male mice were habituated to USV assay arena for three days before testing under red light with control odour (50 µl tonic water). The test arena is a modified home cage with bottom removed and placed inside a larger arena with a glass bottom to also monitor female urine evoked male urine marking behaviour. On test day, behaviour is recorded while subject freely interacts with control odour for 2 min, then 50 µl female urine (collection described below) is added to the chamber and behaviour is recorded for another 2 min. Individuals are then returned to home cage. Behaviour is recorded with a wide-angle camera (Logitech C930e) capture video at 15 frames per second, 640 × 360 pixel resolution and USVs were recorded using a USB microphone (Dodotronic Ultramic250K) both mounted on a customized cage lid. Analogue pulse-controlled LEDs in camera field of view was used to synchronize camera with audio recording. Videos frames were recorded using Adobe After Effects and synched with USV emission using custom MATLAB software. Data were acquired at 196 kHz using SeaWave software and synchronized to video streams with a 4.1 kHz tone (RadioShack Piezo Buzzer, 273-0074) driven by the same analogue pulse used for video synchronization LEDs. Analysis was performed in MATLAB using a modified protocol of Holy and Gao[4]. USV power was calculated as acoustic power in the 40–90 kHz band.

Context or sensory stimuli to evoke USVs. All behaviour was performed in subject's (male) home cage, as adapted from Chabout et al.[30].

Female urine. Adult (8–16 weeks) C57BL/6j female mice were housed five per cage, and soiled male mouse bedding was introduced into the cage 24 h before the first collection night to induce oestrous. The female mice were placed in metabolic cage for 12–16 h overnight, and urine was collected directly into a sterile tube on dry ice and temporarily stored at −20 °C in the morning. Urine was collected for four consecutive nights from four cages (20 mice total), such that the stimulus consisted of a mix from all stages of the oestrous cycle. Urine was then thawed on ice, rapidly passed through a 0.22-µm filter (Millipore Steriflip SCGP00525), aliquoted and stored at −80 °C. Two different batches of urine were collected for all experiments, and each was used with both control and experimental groups. Finally, 100 µl urine was placed on a cotton ball and presented to target male mice for 2 min.

Male urine. Adult (8–16 week) C57BL/6j male mice were housed in pairs before collection. Urine was collected as described for female mice. Urine was pooled from a total of 8 mice. Then, 100 µl urine was placed on a cotton ball and presented to target male mice for 2 min.

Awake female. Adult (8–16 weeks) BALB/cByJ female mice were group housed. Individual female mice were removed from the home cage and introduced to the male resident's home cage. After recording, the female mouse was temporarily held in a clean cage until all cage mates were assayed. Each female interacted with a single male once on daily bases. After each assay, all female mice were returned to their home cage and provided sunflower seeds.

Anaesthetized female or male mice. Wild-type C57Bl/6j mice were sedated with ketamine (10 mg ml^{-1}, Butler Schein) diluted to final concentration of 62.5 mg ml^{-1} in sterile saline and xylazine (20 mg ml^{-1}, AnaSed Injection) to a final concentration of 6.25 mg ml^{-1}, stored at 4 °C for up to two days. A mixture of ketamine and xylazine (1.6 µl mg^{-1} body weight) was administered intramuscularly. Anaesthetized female or male mice were monitored for breath rate and placed on a heating pad before and after testing. Individuals were used in up to four trials then placed in a holding cage. After recovery, individuals were returned to their home cage and provided with sunflower seeds.

Pup USV recording. An individual pup, at postnatal day (P) 7–8 was removed from their home cage[31] and put in the USV assay arena describe above for 5 min while video behaviour and audio emissions were recorded as described above. Pups were then returned to a holding cage with a heating pad after individual recordings. After all pups from the same cage were tested, they were returned to their home cage.

General surgical procedures

Mice were anaesthetized with isoflurane (5% induction, 1–2% maintenance, Kent Scientific SomnoSuite) and placed in a stereotaxic frame (David Kopf Instruments Model 962). Ophthalmic ointment (Puralube) was applied, buprenorphine (Buprenex, 0.15 mg kg^{-1}) was administered intramuscularly at the beginning of the procedure, and 500 µl sterile saline containing carprofen (Rimadyl, 5 mg kg^{-1}) and enrofloxacin (Baytril, 5 mg kg^{-1}) was administered subcutaneously at the end of the procedure. Mice were monitored daily and given at least 14 days for recovery and viral expression before subsequent behavioural testing.

Viral injection or fibre optic implantation

Viral injections were made using pulled glass pipettes (tip inner diameter (ID) 0–20 µm) and a Picospritzer at 35–75 nl min^{-1}. For LPOA injections, a medial-lateral angle of 20° was used to avoid the ventricle. The pipette entry coordinate relative to bregma was 0.1 mm caudal, 2.5 mm lateral, and 4.3 mm diagonally below the dura. Adeno-associated viruses (AAVs) were injected 200–350 nl per side, and the pipette was left in place for 5 min after injection before slowly retracting. For PAG VGAT site injections, the pipette entry coordinate relative to bregma was 4.3 caudal, 0.65 lateral and 2.1 mm below dura. For PAG VGLUT2 (PAG USV-gate neurons) site injections, the pipette entry coordinate relative to bregma was 4.5 caudal, 0.8 lateral and 2.0 mm below dura. For photostimulation, fibre optic implants (4 mm length for PAG and 6mm length for LPOA, Plexon 230 µm diameter for ChR2) were inserted along the pipette track as above, 300 µm above the injection site for ChR2. For fibre photometry implants, 2.5 mm diameter metal ferrule optical cannulas (6 mm fibre length for LPOA and 3 mm length for PAG, MFC_400/430-0.48_MF2.5_FLT Doric lens) were inserted along the pipette track as above, 100 µm above the viral injection site. After injection or implantation, the skull was covered with Metabond (C&B Metabond) and super glue was used to seal the craniotomy and hold the implants in place.

AAV viral vectors

For ChR2 activation, AAV9-CAG-FLEX-ChR2-tdTomato (UPenn AV-9-18917P) was injected bilaterally at 3.5×10^{12} genome copies (GC) per ml in ESR1-Cre/VGAT-Cre/VGLUT2-Cre mice at LPOA cite or unilaterally injected to VGLUT2-Cre mice at the PAG site. For photostimulation controls, same virus was injected bilaterally in ESR1-Cre wild-type litter mates at LPOA site. For DREADD inhibition in wild-type mice, AAVdj-CAG-FLEX-hM4Di-GFP (Addgene plasmid 52536, a gift from S. Sternson) mixed with AAVdj/1-EF1α-FLEX-hM4Di-mCherry (Addgene plasmid 50461, a gift from B. Roth) and AAV9-Cre (UPenn AV-9-PV1090) injected bilaterally at 4×10^{12} GC ml^{-1} in LPOA. For DREADD inhibition in ESR1-Cre mice, AAVdj/1-EF1α-FLEX-hM4Di-mCherry (Addgene plasmid 50461, a gift from B. Roth) was injected to ESR1-Cre mice, and as control, AAV1-CAG-DIO-tdTomato (UPenn, AV-1-ALL864) was injected to either ESR1-Cre or wild-type cage mates bilaterally at the LPOA site. For co-injection with ChR2, only AAVdj/1-EF1α-FLEX-hM4Di-mCherry was injected at PAG in VGAT-Cre mice. For activation of PAG^{VGAT} cells, AAV-hSyn-DIO-hM3Dq-mCherry (Addgene 44361, a gift from B. Lim) was injected bilaterally to PAG in VGAT-Cre mice. As a control, AAV1-CAG-DIO-tdTomato (UPenn, AV-1-ALL864) was injected in VGAT-Cre mice. For anatomy tracing, RG-EIAV-CAG-DIO-Flp (a gift from B. Lim) was injected unilaterally in ESR1-Cre mice at the PAG site while AAV-EF1α -fDIO-eGFP was injected to LPOA. For labelling PAG-USV cells projecting to the nucleus ambiguous, AAV-retro-hSyn-eGFP (a gift from B. Lim) was injected into the nucleus ambiguous at 4×10^{12} GC ml^{-1}. For fibre photometry, AAV1-CAG-DIO-GCaMP6s (UPenn, AV-1-PV2818) was mixed with AAV9-CAG-DIO-GCaMP6s (UPenn, AV-9-PV2818) and diluted to 5×10^{12} GC ml^{-1}, then mixed virus was injected bilaterally into LPOA site in ESR1-Cre mice. For co-injection with ChR2, the same virus was injected to PAG site unilaterally in VGAT-Cre mice.

ChR2 stimulation

For photostimulation experiments, fibre-implanted mice were handled gently by hand to connect and disconnect patch cables (Plexon 0.5 m, 230 μm 68 diameter). An LED current source (Mightex BLS-SA02-US) driving two 465 nm PlexBright Compact LED Modules (Plexon) through a Dual LED Commutator (Plexon) provided 8 ± 1 mW exiting the fibre tips. Optical power was measured (ThorLabs PM20A) before and after each session. Mice were placed in the recording box (identical to home cage with bottom removed[6]). For dose–responses curve (Figs. 3h, 4a), photostimulation occurred for 5-s duration using 15-ms pulses at five different frequencies: 1, 5, 10, 25, 50, 50, 25, 10, 5 and 1 Hz for test day 1, and 50, 25, 10, 5, 1, 1, 5, 10, 25 and 50 Hz for test day 2. At least 40 s elapsed between different photostimulation frequency, with delays occasionally occurring when the mouse reared towards the cage top, to avoid variabilities of sound amplitude. Forty seconds was on the basis of pilot experiments to determine maximum USV bout length after USVs emitted after a single stimulation. For time dose testing, mice were given 25 and 50 Hz, 15-ms pulses for 1 s, 5 s, 10 s and 20 s duration with at least 1 min between stimulation. In addition, 12 mice that were bilaterally infected in the $LPOA^{ESR1}$ neurons with ChR2 virus were tested for unilateral or bilateral stimulation comparison with all test conditions. The same dose curve and time dose curve stimulation parameter was used to test the left and right side separately (no quantitative difference was found so these mice were pooled for the final analysis). For optogenetic stimulation on PAG^{VGLUT2} cells, the dose curve starts with 1 Hz and stopped at 10 Hz because at greater stimulation frequencies, these individuals demonstrated additional ballistic movement behaviours as previously described[17]. At stimulation frequencies starting with 25 Hz, we also observed that mice displayed tail rattling as well as freezing behaviour. Time of stimulation was manually recorded by playback of videos using Adobe After Effects and USV recording subsequently analysed using custom MATLAB software. USV audio files were de-noised and the number of USVs was calculated using MATLAB script previously described[4]. The inter USV interval was calculated on the basis of the difference in time points of each syllable detection by MATLAB code. After all experiments, mice were perfused and analysed for viral expression and fibre placement and immunohistochemistry. Mice that did not have more than 3 syllables emitted under any ChR2 stimulation conditions are excluded from this study (3 out of 26 for $LPOA^{ChR2}$ stimulation, and 3 out of 6 for $PAG^{VGLUT2/ChR2}$ stimulation). For photostimulation in VGAT-Cre mice at the LPOA site, the same photostimulation parameter was used. However, we have observed a delayed USV emission compare to photostimulation in ESR1-Cre mice. In some cases, the USV emission started locked to the end of light stimulation, especially during strong stimulation conditions (25 Hz, 50 Hz).

Rabies tracing

Helper virus[32,33] (AAV-EF1α-DIO-mRuby2-TVA and AAV-EF1α-DIO-oPBG, a gift from B. Lim) was mixed as a 1:1 ratio and injected into the PAG of mice with positive expression of either VGAT-ZsGreen or VGLUT2-ZsGreen. After 2 weeks of expression, EnvA-RVΔG-tdTomato (a gift from B. Lim) was injected in the same injection site. For RNAScope multiplex in situ hybridization experiments, EnvA-RVΔG-eGFP (a gift from B. Lim) was injected into the PAG using VGAT-Cre mice. Mice were perfused 5 days after rabies virus injection and brain sections were processed for imaging.

DREADD inhibition or activation

After hM_4D_i or hM_3D_q viral injection, mice were allowed at least 21 days for recovery and expression, and then intraperitoneally injected 50–60 min before testing with control saline plus 0.5% DMSO or CNO (5 mg kg^{-1}, Enzo Life Sciences BML-NS105-0025) in saline plus 0.5% DMSO. For wild-type or ESR1-Cre mice with hM_4D_i injections into the LPOA, injections of control saline or CNO were performed on alternative days before female urine was given. Mice received the following injections 45–55 min before behaviour testing: day 1 = CNO; day 2 = saline; day 3 = CNO; day 4 = saline; and day 5 = CNO. In the home cage of test mice, 2 min of background USVs were recorded, a female was introduced to the home cage of the male mouse for 3 min, and the female mouse was subsequently returned to her home cage. To combine ChR2 stimulation with DREADD inhibition or activation, mice were first tested for ChR2 stimulation alone as described above (see 'ChR2 stimulation' section). Two days later, each mouse was tested for ChR2 stimulation 45–55 min after an intraperitoneal injection of either CNO or saline (day 1 = CNO; day 2 = saline; day 3 = CNO; day 4 = saline; and day 5 = CNO). The number of USVs was counted using the MATLAB script written in house.

Social behaviour scoring

To determine the social response of male mice to a behaving female mouse (Extended Data Fig. 2l), an unbiased blinded individual scored mouse behaviour by playback of the videos recorded from the side of test cages. The following behaviours were scored each second for 4 min after the first exposure to a live female and reported in an Excel sheet: sniff the female mouse (any part except for anogenital region; anogenital sniff (male mouse's nose in female anogenital region); mount attempt (male on top of female); female aggressive behaviour (typified by female sitting upright or audible vocalizations; self-grooming; and digging. The total amount of time each mouse spent on each behaviour was calculated between test conditions.

Fibre photometry

Mice recovered from surgery for at least three weeks before testing. Bulk GCaMP signals (470 nm excitation) as well as the isosbestic control channel (405 nm excitation) were collected at 20 Hz in alternation as previously described[34]. Signals were recorded using the previously developed MATLAB GUI[34]. A pulse was sent to an LED light by the data acquisition board with the start of the GUI. GCaMP signals were synchronized with USV audio files using similar methods to that described

in the USV recording sections as applied to USV audio and video files. The video files were synchronized to GCaMP signals using an LED light triggered by the data acquisition board. Mice were first recorded for 4 min in their home cage, then a live female mouse was introduced to their home cages for another 4–5 min. After freely interacting with the female mouse, she was removed from the home cage of the test mouse and post-female USVs were recorded for an additional 4–5 min. $\Delta F/F$ values were calculated using the previously developed MATLAB GUI[34]. We used methods similar to those described in 'USV analysis' to detect USVs in the audio file. Using the USV time points, we selected GCaMP signals at corresponding time points for analysis. Each mouse went through several days of recording with pre-female, with-female and post-female stages per test day where each day was a trial. Trials were excluded if there were indications that the fibre connection was poor as indicated by a GCaMP signal that failed to increase above the threshold of 1.5% $\Delta F/F$ during the entire recording of that particular test day (17 out of 118 trials were excluded for the $LPOA^{ESR1}$ fibre photometry data and 0 trials were excluded for the PAG^{VGAT} fibre photometry with $LPOA^{VGAT}$ photostimulation). The dataset consisted of GCaMP traces that were sectioned by −30 s and +30 s around USV onset. High-pass filters were applied to GCaMP windows as necessary to remove slow drift by subtracting a smoothed version of the signal from itself in rolling windows. Traces were then normalized via *z*-scoring using the standard deviation and mean of the signal before −10 s for each section. The dot plots comparing average GCaMP signal at no-USV time points versus USV time points were produced by using the mean GCaMP signal around the 150 ms window (−75 ms, +75 ms) at each USV onset. The mean of each group was then taken to produce the shown data points. To create data for the no-USV group, random time points from each GCaMP signal in the USV group were chosen using the same number of USVs detected for each sample. To calculate whether the differences between groups were statistically significant, we used a two-tailed unpaired *t*-test. The average GCaMP line plot was produced using a window of −30 s and +30 s from all detected USVs in each group, and the shaded boundary along the mean represents the 95% confidence interval. The grey area represents the estimated shuffle distribution, calculated by scrambling the GCaMP traces 1,000 times, computing the means, and using the 97.5th percentile of the absolute value as the confidence interval. For fibre photometry recording performed together with photo stimulation, $\Delta F/F$ was calculated 10 s before and after light stimulation period and plotted as grouped data similar to the average line plot described above. For fibre photometry recording performed together with photo stimulation, *z*-score was calculated 10 s before and after light stimulation period using 'zscore' function in MATLAB and plotted as grouped data with shading zone indicates the 95% confidence interval.

Vibratome and ESR1 staining

Mice were perfused with cold PBS followed by 4% paraformaldehyde (PFA), and the brain was dissected and post-fixed in 4% PFA at 4 °C for 24–48 h. The brain was then washed in PBS and embedded in 1% low melting point agarose and cut on a vibratome at 50um for ESR1 and/or FOS staining or 100 μm for Nissl-only staining. For ESR1 immunostaining, free-floating sections were blocked in 1% BSA (Sigma A3059) in 1% PBST (PBS plus Triton X-100) for 3 h, followed by primary incubation with anti-ESR1 antibody (Millipore, oestrogen receptor alpha, rabbit, 06935MI) diluted 1:1,500 in 1% BSA, 0.3% PBST) overnight at 4 °C. Sections were then washed in 0.1% PBST six times, 5 min each on the second day before incubation with secondary antibody (ThermoFisher Alexa-Fluor 488 or 647 anti-rabbit IgG H+L diluted 1:2,000 in 1% BSA, 0.3% PBST) at room temperature for 3 h. Nissl stain (ThermoFisher NeuroTrace Blue or Deep Red diluted 1:200) was also included if necessary, or incubated for 4 h in 1% PBST if used alone. Sections were washed four times in 0.1% PBST, followed by two washes in 1× PBS, then mounted with ProLong Diamond (ThermoFisher).

Multiplex fluorescent in situ hybridization (RNAscope)

Mice were anaesthetized with isoflurane and perfused with 1× PBS before rapid brain extraction. Brains were embedded in OCT and frozen on dry ice immediately. Coronal sections (20 μm) were cut via a Cryostat (Leica) and stored at −80 °C until processing according to the protocol provided in the RNAscope Multiplex Fluorescent v2 kit (Advanced Cell Diagnostics). Sections were fixed in 4% PFA, dehydrated and hybridized with mixed probes: ESR (Mm-ESR1-O2-C2, a 16ZZ probe targeting 1308-2125 of NM_007956.5.), eGFP (Cat. 538851), VGAT (Mm-Slc32a1, 319191), and VGLUT2 (Mm-Slc17a6-C2, 319171) for 2 h at 40 °C and followed by amplification. Signal in each channel was developed using TSA cyanine 3, fluorescein, and cyanine 5 (PerkinElmer) individually. Sections were counterstained with DAPI and mounted with ProLong Diamond.

Confocal microscopy

Images were captured with a Nikon A1 Confocal Microscope with a 10× air or 20× air objective. Nikon Elements software settings were optimized for each experiment to maximize signal range, and *z*-stack maximum projections were used for quantification, while single optical slices were used for representative images. For RNAScope multiplex in situ hybridization, *z*-stacks were collected in 1-μm increments throughout the *z*-axis.

Slice electrophysiology

Mice were anaesthetized with isoflurane and transcardially perfused with ice-cold choline-based slicing solution, containing (in mM): 25 $NaHCO_3$, 1.25 NaH_2PO_4, 2.5 KCl, 7 $MgCl_2$, 25 glucose, 0.5 $CaCl_2$, 110 choline chloride, 11.6 sodium ascorbate, and 3.1 sodium pyruvate. Brains were carefully extracted and transferred to a chamber filled with the same solution on a vibratome (VT1200; Leica). Brains were coronally sliced at 250 μm and incubated at 35 °C for 15–20 min in recovery solution, containing (in mM): 118 NaCl, 2.6 $NaHCO_3$, 11 glucose, 15 HEPES, 2.5 KCl, 1.25 NaH_2PO_4, 2 sodium pyruvate, 0.4 sodium ascorbate, 2 $CaCl_2$ and 1 $MgCl_2$. Slices were maintained at room temperature for at least one hour until transferred to a recording chamber on an Olympus BX51WI upright microscope. The chamber was continuously superfused with artificial cerebrospinal fluid (ACSF), containing (in mM): 125 NaCl, 25 $NaHCO_3$, 2.5 KCl, 1.25 NaH_2PO_4, 11 glucose, 1.3 $MgCl_2$, and 2.5 $CaCl_2$, maintained at 30 ± 2 °C by a feedback temperature controller. Slicing solution, recovery solution, and ACSF were constantly bubbled with 95% O_2 and 5% CO_2. All compounds were purchased from Tocris or Sigma.

For all recordings, patch pipettes (3–5 MΩ) were pulled from borosilicate glass (G150TF-4; Warner Instruments) with a DMZ Universal Electrode Puller (Zeitz Instruments) and filled with appropriate intracellular solutions. Liquid junction potential was not corrected for any experiments. Neurons were visualized with differential interference contrast optics or epifluorescence (Olympus). Recordings were made with a MultiClamp700B amplifier and pClamp10 software (Molecular Devices). Data were low-pass filtered at 1 kHz and digitized at 10 kHz with a digitizer (Digidata 1440; Molecular Devices). Series resistance was monitored and cells that displayed a more than 20% change over the duration of recording were excluded.

To record optogenetically evoked postsynaptic currents in PAG neurons, pipettes were filled with Cs-based intracellular solution, containing (in mM): 115 Cs^+-methanesulfonate, 10 HEPES, 1 EGTA, 1.5 MgCl2, 4 Mg^{2+}-ATP, 0.3 Na^+-GTP, 10 Na_2-phosphocreatine, 2 QX 314-Cl, 10 BAPTA-tetracesium (295 mOsm, pH 7.35). ChR2-expressing axon terminals were stimulated with a 5-ms blue light pulse emitted from a collimated light-emitting diode (473 nm; Thorlabs) driven by a T-Cube LED Driver (Thorlabs) under the control of Digidata 1440A Data Acquisition System and pClamp10 software (Molecular Devices). Light was delivered through the reflected light fluorescence illuminator port and the 40× objective at maximum intensity (13.45 mW). Before break-in, recordings were performed in a cell-attached configuration

with trains of 5-, 10-, 25- or 50--Hz light pulses. Recordings of optogenetically evoked excitatory postsynaptic currents (EPSCs) or IPSCs were then obtained from the same cells in voltage-clamp configuration. We measured EPSCs around −60 mV and IPSCs around 5 mV[35]. Spikes and EPSCs or IPSCs were analysed using a custom Python script.

For current-clamp recording, pipettes were filled with an intracellular solution containing (in mM): 125 K^+-gluconate, 4 NaCl, 10 HEPES, 0.5 EGTA, 20 KCl, 4 Mg^{2+}-ATP, 0.3 Na^+-GTP, and 10 Na_2-phosphocreatine (290–300 mOsm, pH 7.2). To measure optogenetially evoked firing of LPOA neurons, recordings were performed with similar photostimulation protocol (trains of 5, 10, 25, or 50-Hz light pulses). All current-clamp recordings were performed in the presence of 5 μM NBQX and 50 μM picrotoxin to block synaptic transmission.

MUPET analysis

We applied a high-pass wavelet filter to allow only 40-kHz frequencies and higher in recording files. Default MUPET settings were used in processing, except for noise suppression set to 10 before inputing the files to MUPET. To build repertoires, we empirically chose 40 syllables to analyse, as previously described[15].

USV analysis

We began by filtering the recordings for each trial, excluding frequencies that were below 40 kHz or above 90 kHz to reduce the non-USV noise. To calculate USV power, the power spectrum of the raw data (Dodotronic Ultramic UM250K) was calculated using the 'spectrogram' function in MATLAB. Power in the 40–90 kHz band was converted to decibels using a reference power of 10×10^{-12} W, and room noise less than 1.5 s.d. above mean power was subtracted. This power signal was then smoothed with a 50-ms Gaussian window, and total power is reported as the integration of the smoothed power trace using the 'trapz' function. MATLAB 'findpeaks' (minimum peak amplitude of 1 s.d. above noise, minimum peak separation 150 ms) was applied to the smoothed power trace to count the number of USVs. For the average USV power plot, we plotted the mean of all the trials, as well as the 95% confidence interval for the mean (calculated as 1.96 times the s.e.m.).

For syllable classification, we first computed the short-time Fourier transform (STFT) of the microphone trace using a multi-taper approach. Spectrograms were computed using Slepian tapers with a time-halfbandwidth product of 3, and the amplitude of the STFT was then log-transformed. To detect ultrasonic vocalizations (USVs) we used similar approach to that previously described[4]. In brief, we computed the USV power (30–90 kHz), spectral contrast, and Wiener entropy, and used empirically determined thresholds to detect USV calls while filtering out noise. To classify calls, STFTs were dimensionally reduced using principal components analysis (PCA). The resulting PCA scores (27 principal components explaining 90% of the variance were retained) were then modelled with a hidden Markov model with Gaussian emissions. The discrete states of the model were used for classification.

Cell count

After selecting a rectangular region of interest median or gaussian filters are applied. On the basis of an intensity threshold for a dataset, the image is binarized into black and white. All objects with fewer than threshold pixels are removed from the image where threshold pixels determined by the resolution of the images in the data set to best describe the size of cells. To prevent over segmentation, the image is dilated, and connected components are shrunk to individual points. Then we count the number of components in the image. The coordinates of those cells within a region of interest are then converted into a scatter plot or heat map.

Reporting summary

Further information on research design is available in the Nature Research Reporting Summary linked to this paper.

Data availability

The data in this study are available from the corresponding author upon request. Source data are provided with this paper.

Code availability

All analysis code are available on GitHub: https://github.com/stowerslab/USV_Analysis_Code.git.

30. Chabout, J., Jones-Macopson, J. & Jarvis, E. D. Eliciting and analyzing male mouse ultrasonic vocalization (USV) songs. *J. Vis. Exp*. https://doi.org/10.3791/54137 (2017).
31. Yin, X. et al. Maternal deprivation influences pup ultrasonic vocalizations of C57BL/6J mice. *PLoS ONE* **11**, e0160409 (2016).
32. Cetin, A. & Callaway, E. M. Optical control of retrogradely infected neurons using drug-regulated "TLoop" lentiviral vectors. *J. Neurophysiol*. **111**, 2150–2159 (2014).
33. Knowland, D. et al. Distinct ventral pallidal neural populations mediate separate symptoms of depression. *Cell* **170**, 284–297 (2017).
34. Kim, C. K. et al. Simultaneous fast measurement of circuit dynamics at multiple sites across the mammalian brain. *Nat. Methods* **13**, 325–328 (2016).
35. Xue, M., Atallah, B. V. & Scanziani, M. Equalizing excitation-inhibition ratios across visual cortical neurons. *Nature* **511**, 596–600 (2014).
36. Hurst, J. L. & Beynon, R. J. Scent wars: the chemobiology of competitive signalling in mice. *BioEssays* **26**, 1288–1298 (2004).
37. Nyby, J. et al. Stimuli for male mouse (Mus musculus) ultrasonic courtship vocalizations: presence of female chemosignals and/or absence of male chemosignals. *J. Comp. Physiol. Psychol*. **95**, 623–629 (1981).
38. Reynolds, E. Urination as a social response in mice. *Nature* **234**, 481–483 (1971).
39. Gordon-Fennell, A. G. et al. The lateral preoptic area: a novel regulator of reward seeking and neuronal activity in the ventral tegmental area. *Front. Neurosci*. **13**, 1433 (2020).
40. Hileman, S. M., McManus, C. J., Goodman, R. L. & Jansen, H. T. Neurons of the lateral preoptic area/rostral anterior hypothalamic area are required for photoperiodic inhibition of estrous cyclicity in sheep. *Biol. Reprod*. **85**, 1057–1065 (2011).
41. Ono, T., Nakamura, K., Nishijo, H. & Fukuda, M. Hypothalamic neuron involvement in integration of reward, aversion, and cue signals. *J. Neurophysiol*. **56**, 63–79 (1986).
42. Osaka, T. et al. Lateral preoptic neurons inhibit thirst in the rat. *Brain Res. Bull*. **31**, 135–144 (1993).
43. Szymusiak, R., Gvilia, I. & McGinty, D. Hypothalamic control of sleep. *Sleep Med*. **8**, 291–301 (2007).
44. Pomerantz, S. M., Nunez, A. A. & Bean, N. J. Female behavior is affected by male ultrasonic vocalizations in house mice. *Physiol. Behav*. **31**, 91–96 (1983).
45. Sangiamo, D. T., Warren, M. R. & Neunuebel, J. P. Ultrasonic signals associated with different types of social behavior of mice. *Nat. Neurosci*. **23**, 411–422 (2020).
46. Neunuebel, J. P., Taylor, A. L., Arthur, B. J. & Egnor, S. E. Female mice ultrasonically interact with males during courtship displays. *eLife* **4**, (2015).
47. Kohl, J. & Dulac, C. Neural control of parental behaviors. *Curr. Opin. Neurobiol*. **49**, 116–122 (2018).
48. Tan, C. L. & Knight, Z. A. Regulation of body temperature by the nervous system. *Neuron* **98**, 31–48 (2018).
49. Yu, S., François, M., Huesing, C. & Münzberg, H. The hypothalamic preoptic area and body weight control. *Neuroendocrinology* **106**, 187–194 (2018).
50. Jürgens, U. The role of the periaqueductal grey in vocal behaviour. *Behav. Brain Res*. **62**, 107–117 (1994).
51. Jürgens, U. The neural control of vocalization in mammals: a review. *J. Voice* **23**, 1–10 (2009).
52. Bandler, R. & Shipley, M. T. Columnar organization in the midbrain periaqueductal gray: modules for emotional expression? *Trends Neurosci*. **17**, 379–389 (1994).
53. Inagaki, H. K. et al. Optogenetic control of *Drosophila* using a red-shifted channelrhodopsin reveals experience-dependent influences on courtship. *Nat. Methods* **11**, 325–332 (2014).

Acknowledgements We thank the Stowers laboratory for support and advice; T. Holy and T. Barnes for early constructive comments and discussions; S. Tan, N. Koblesky and S. Simpson for exploratory behavioural tests; and L. Ye for aid with the fibre photometry experiments. The work was supported by the Dorris Neuroscience and Skaggs Scholarships (J.C.) the Anandamahidol Foundation Fellowship (V.L.), Career Award at the Scientific Interface from BWF (J.E.M.), and grants from NIH (R01NS097772 and R01DA049787 (B.K.L.); and R01NS108439 (L.S.)).

Author contributions J.C. and L.S. designed the study and wrote the manuscript. J.E.M. and S.R.D. developed Voseq analysis; V.L. performed slice physiology; S.T. aided in histology, behavioural testing and cell counting; B.K.L., P.S. and J.A.K. aided in data analysis and MATLAB code. J.R.J. performed behavioural analysis. All other experiments were performed by J.C.

Competing interests The authors declare no competing interests.

Additional information

Supplementary information The online version contains supplementary material available at https://doi.org/10.1038/s41586-021-03403-8.

Correspondence and requests for materials should be addressed to L.S.

Peer review information *Nature* thanks Erich Jarvis and the other, anonymous, reviewer(s) for their contribution to the peer review of this work. Peer review reports are available.

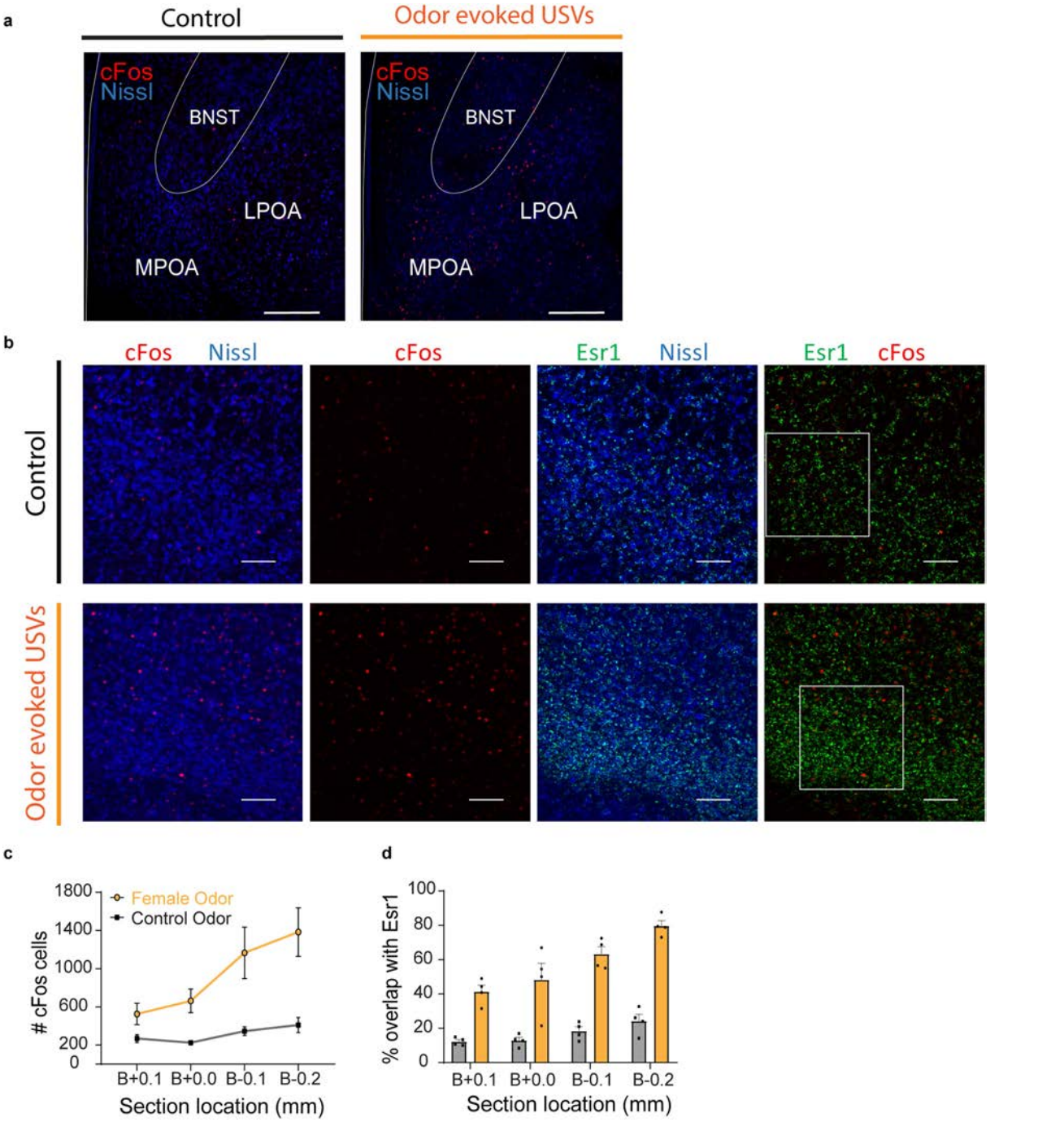

Extended Data Fig. 1 | ESR1-expressing subset of LPOA neurons express c-FOS during odour-evoked USV calling. a, Example of c-FOS expression in the preoptic area after exposure to tonic water as a control odour (no USVs) or with female odour (USVs)[25,36–38]. Scale bar, 200 µm. Quantification of this experiment is shown in **c** and **d**. **b**, Immunostaining after exposure to female mouse odour shows that c-FOS$^+$ in the LPOA largely overlaps with ESR1-ZsGreen cells. White squares delineate enlarged single *z*-stack sections shown in Fig. 1b. Scale bar, 100 µm. **c**, **d**, Expression of c-FOS and ESR1 in the LPOA following awake behaviour with control odour (black) or female odour (yellow). **c**, Rostrocaudal distribution of c-FOS$^+$ cells in the LPOA. **d**, Rostrocaudal percentage of cells co-expressing c-FOS and ESR1 in the LPOA. Data are mean ± s.e.m. $n = 4$ mice.

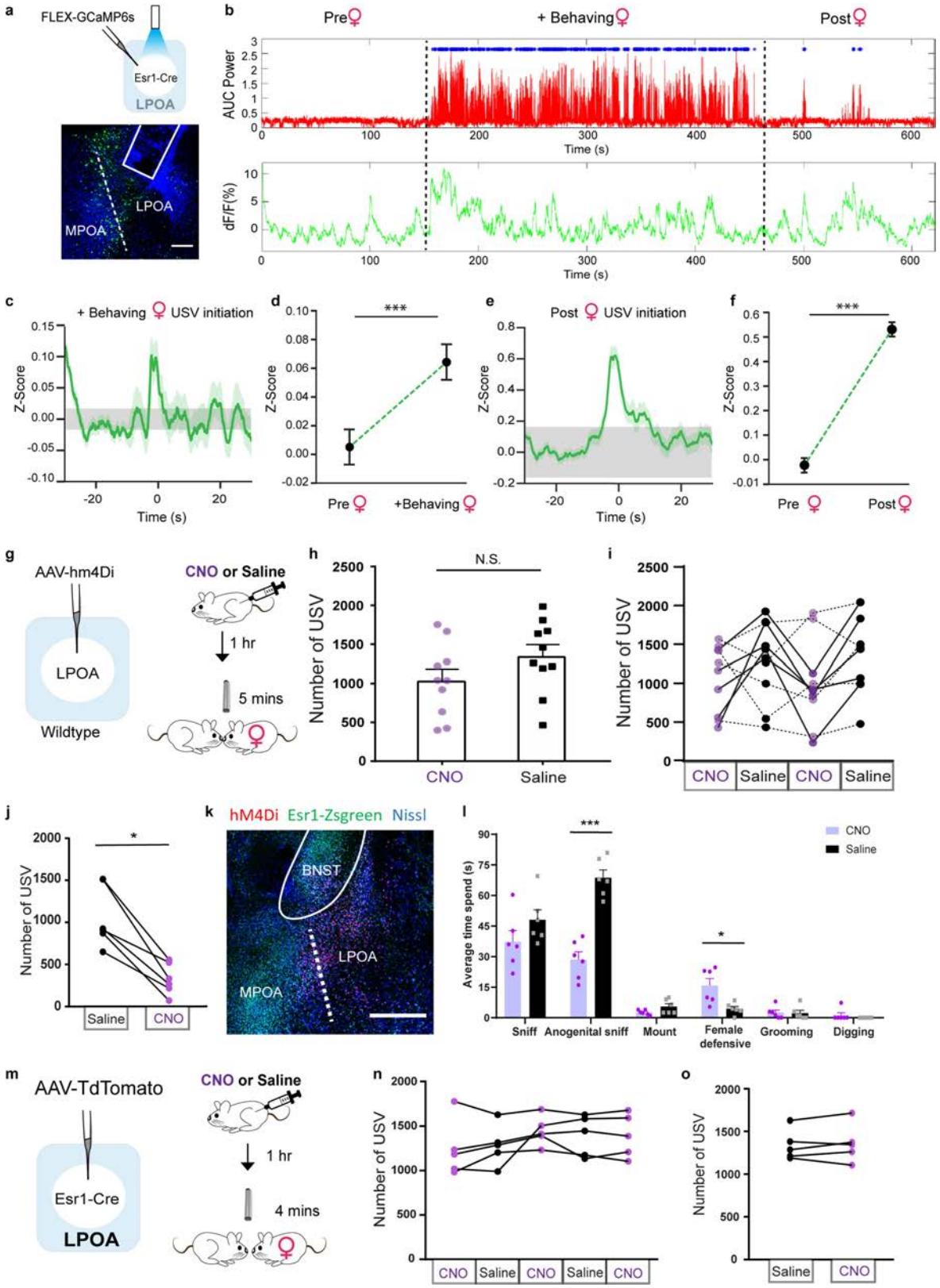

Extended Data Fig. 2 | See next page for caption.

Extended Data Fig. 2 | LPOA^{ESR1} neural activity correlates with USV calling, and chemogenetic inhibition of LPOA^{ESR1} neurons reduce USV calling. LPOA^{ESR1+} GCaMP6s activity during natural social behaviour. **a**, Top, experimental design for LPOA^{ESR1} fibre photometry recordings. Bottom, sample image showing fibre optic track and viral expression of GCaMP6s. Scale bar, 200 µm. $n = 9$ mice, >3 sections per mouse collected. In addition to evoking USV calling, the presence of a female mouse also markedly alters the behaviour of the male mouse (arousal, social sniffing, locomotion and sexual mounting), potentially confounding interpretation of the observed neural activity. We observed that after the removal of the female mice, male mice often generated intermittent USV calls, perhaps to lure the female mice back, without the behavioural noise of mounting or social sniffing. We leveraged this post-female period to observe increases in LPOA$^{ESR1/GCaMP6s}$ activity with a rise shortly before the onset of post-female USVs, clearly suggesting that endogenous LPOA^{ESR1} neural activity correlates with emission of USVs. **b**, Representative USV production and GCaMP6s fibre photometry of male LPOA^{ESR1} neurons as he behaves alone (pre-female), with a behaving female mouse, and after the female mouse is removed (post-female). Dashed line indicates when the female was added and removed. Top, mean USV power. Blue dots indicate USV syllable detection. Bottom, $\Delta F/F$ of LPOA^{ESR1} GCaMP6s signals was calculated by MATLAB GUI as previously described[34]. **c**, Dark green line denotes mean z-score of GCaMP6s signals before and after initiation of USV with behaving female phase, light green shading indicates 95% confidence interval. Grey shading denotes 95% confidence interval of the mean of the scrambled data ($n = 9$ mice). **d**, Mean average z-score of GCaMP6s signals during all USV syllables evoked with a behaving female compared to scrambled data points during pre-female behaviour. Data are mean ± s.e.m. $n = 9$ mice. $^{***}P = 0.0003$, unpaired t-test, two sided. **e**, Dark green line denotes mean z-score of GCaMP6s signals before and after initiation of USV during post-female stage, light green shading indicates 95% confidence interval. Grey shading denotes 95% confidence interval of the mean of the scrambled data. $n = 9$ mice. **f**, Mean average z-score of GCaMP6s signal of all USV syllables during post-female stage compared to scrambled data points during pre-female stages. Data are mean ± s.e.m. $n = 9$ mice. $^{***}P = 2.2 \times 10^{-4}$, unpaired t-test, two sided. **g**–**i**, To determine whether the increased hypothalamic activity is involved in odour-evoked USV calling, we targeted chemogenetic inhibition to the LPOA, which is a largely unstudied heterogeneous region that has been implicated in sleep, thirst and reward behaviour[39–43], and quantified USV production during natural interactions with an awake female. **g**, Non-specific chemogenetics. Left, hM_4D_i viral injection in the LPOA of wild-type mice. Right, experimental assay; after expression of the hM_4D_i virus, male mice were injected intraperitoneally with CNO–saline–CNO–saline (every other day for 4 days in total) and allowed to interact with a freely moving female mouse to evoke USV calling. **h**, Number of USV syllables emitted after injection with CNO (purple) or saline (black). Data are mean ± s.e.m. $n = 10$ mice. N.S., $P = 0.11$, paired two-tailed Wilcoxon test. **i**, Number of USVs emitted across four sequential test days. Overall, the manipulation did not produce a significant effect on behaviour; however, half of this group (solid lines, $n = 5$ mice) did show a constant reduction in USVs, whereas the other half (dashed lines, $n = 5$ mice) continued to emit USVs in the presence of CNO. This experiment suggests the potential for a functional role of the hypothalamic neurons in social vocal communication and a need for a more specific viral labelling method. **j**, Average number of USVs between all saline and CNO injection days as shown in Fig. 1d. $n = 6$ mice. $^{*}P = 0.03$, two-sided Wilcoxon test. **k**, Sample image of hM_4D_i expression in ESR1-ZsGreen mice. Scale bar, 500 µm. $n = 6$ mice, >3 sections per mouse collected. **l**, Quantification of total time performing social behaviours observed by LPOA$^{ESR1/hM4Di}$ neurons from male mice during a 4-min interaction with live female mice on CNO and saline injection days. $n = 6$ mice. $^{*}P = 0.02$, $^{***}P < 0.001$, paired two-sided t-test. Note that we observed an unexpected increase in the anti-social defensive behaviour of the female mouse (kicking, running away), which reduced the ability of the male mouse to direct sniffing to the anogenital region. This observation is consistent with male USVs serving to enhance female courtship behaviour[44,45]. **m**, Experiment design to express control AAV-tdTomato virus in LPOA^{ESR1} cells. **n**, Number of USVs emitted with behaving female mice over five test days, with alternating injections of either CNO or saline. **o**, Average number of USVs between saline and CNO injection days. $n = 5$ mice. $P > 0.05$, two-sided Wilcoxon test.

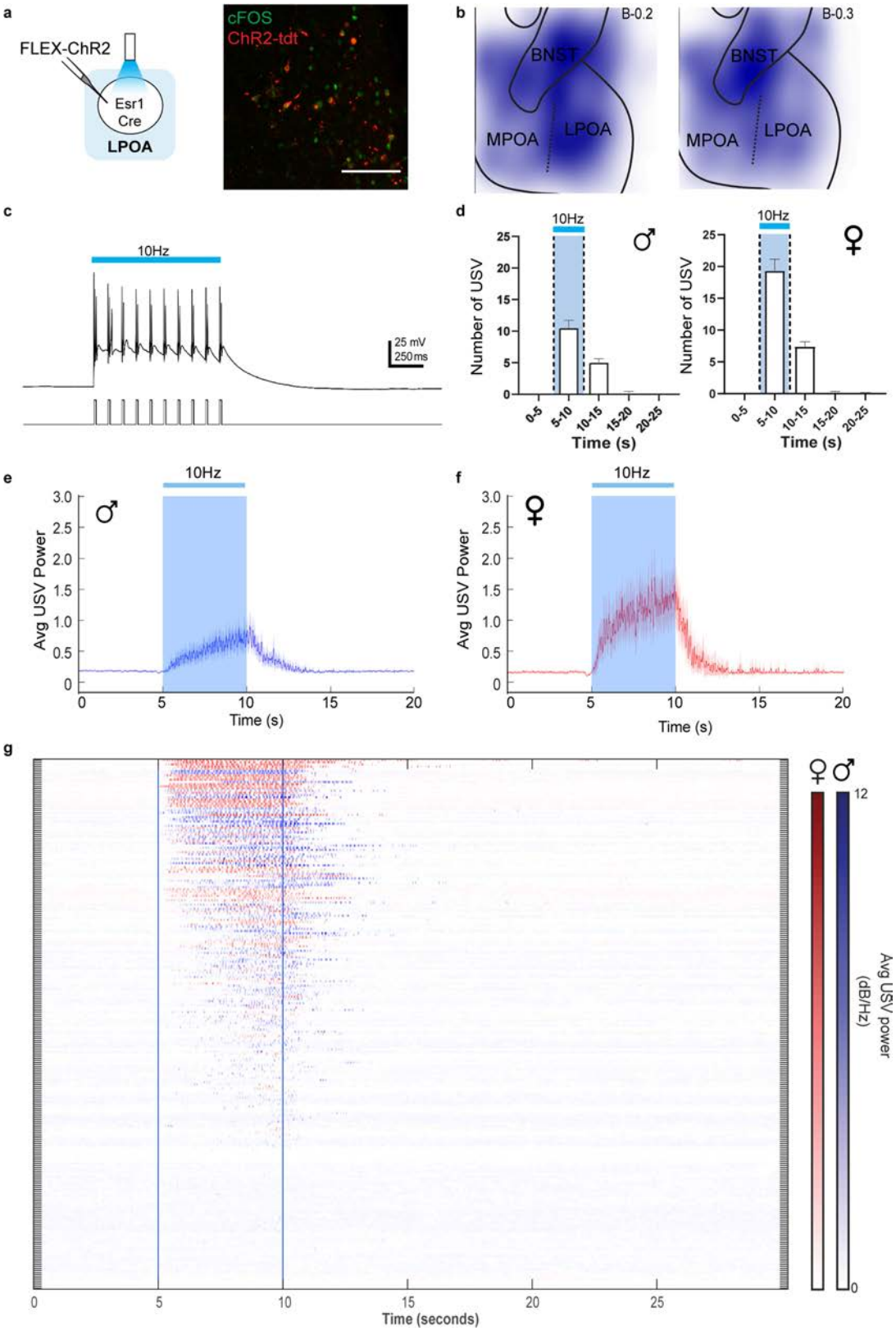

Extended Data Fig. 3 | See next page for caption.

Extended Data Fig. 3 | Optogenetic stimulation of LPOA$^{ESR1/ChR2}$ neurons triggers USV calling in both male and female mice. a, Left, ChR2 virus injection in the LPOA region of ESR1-Cre mice. Right, sample image of co-expression of ChR2 and FOS after photostimulation. Scale bar, 50 µm. **b**, Viral expression in the LPOA region. Composite overlay of total sections at left: bregma 0.2 mm, and right: bregma 0.3 mm. Colour intensity scales with increasing expression. $n = 12$ mice. **c**, Example electrophysiology recording during photostimulation of LPOA$^{ESR1/ChR2}$ neurons in ex vivo slice. Blue bar denotes 10-Hz light stimulation. Neural response is time-locked to light pulses. **d**, Number of USVs detected during 10-Hz photostimulation of LPOA$^{ESR1/ChR2}$ cells from male mice ($n = 23$ mice) (left) and female mice ($n = 11$ mice) (right). Data are mean ± s.e.m. **e**, **f**, Average USV power across the 40–90kHz band evoked by 10-Hz photostimulation. Solid line indicates mean of all trials; shaded region indicates 95% confidence interval. The blue (**e**) and red (**f**) traces denote male and female trials, respectively[14,46]. Blue shaded bar denotes light stimulation at 5–10 s. **g**, Raster plot of complete dataset showing USV power evoked by photostimulation at 10 Hz (5-s duration, 15-ms pulses; between the blue lines) of LPOA$^{ESR1/ChR2}$ neurons from female mice ($n = 11$ mice, red) and male mice ($n = 23$ mice, blue). $n = 242$ trials, each row is a single trial. Colour intensity represents average USV power across the ultrasonic band (40–90 kHz). Note that the POA has been implicated in a variety of functions including homeostatic control of internal states such as thermoregulation and thirst, sexually dimorphic social behaviours including parenting and mating behaviour, as well as motivated behaviours[39,47–49]. It is likely that features of these neurons that enable them to generate USVs in the absence of social stimuli in the laboratory also enable them to participate in other neural computations that are currently unknown.

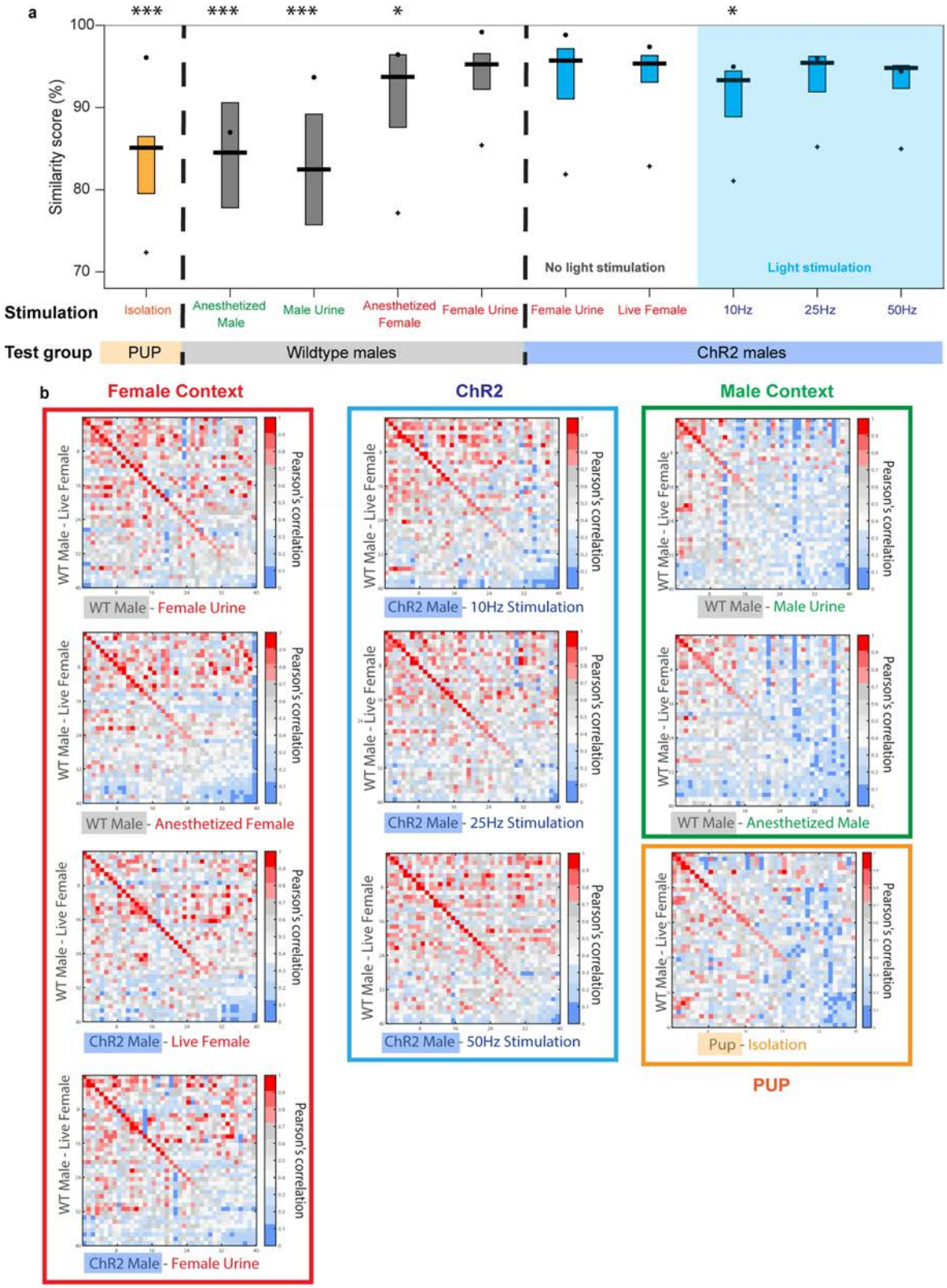

Extended Data Fig. 4 | See next page for caption.

Extended Data Fig. 4 | Activating LPOA^{ESR1} neurons elicit a variety of USV syllables similar to natural USVs. a, Evaluation of USV syllable types emitted by a wild-type male mouse naturally interacting with a behaving female mouse, compared to wild-type P7–P8 pup calls ($n = 18$ mice) (orange) evoked by individually isolating mice from the home cage; wild-type adult male calls ($n = 20$ mice) evoked by interaction with female or male urine, anaesthetized male or female mice on successive days (grey); or calls from experimental male mice expressing ChR2 (LPOA$^{ESR1/ChR2}$, $n = 23$ mice) evoked by interaction with either female urine or a live female mouse with no ChR2 light stimulation to determine the natural USV repertoire (blue, left); or male mice expressing ChR2 (LPOA$^{ESR1/ChR2}$, $n = 23$ mice) stimulated with light (10 Hz, 25 Hz and 50 Hz) in the absence of a female mouse (blue, right; blue shading 'light stimulation'); the same male mice were used in the no-light and light stimulation experiments. Dot denotes the Pearson correlations for the top 5% of the most frequently used syllables, in which the box plot shows the mean and interquartile range of these correlations, and the plus symbol ('+') shows the correlation of the top 95% of the most frequency used syllables. $P = 6.12 \times 10^{-115}$ ($F > 83.4$), $^{*}P < 0.05$, $^{***}P < 0.001$, one-way ANOVA test. MATLAB 'mulcompare' function was used for group statistical analysis comparing all other groups to wild-type male USV triggered by interaction with a live female mouse. **b**, Heat map showing Pearson's correlation score among all 40 types of syllable detected across each condition compared to wild-type male USVs during interaction with live female mouse. Results are grouped by types of sensory stimulation: female context (red); ChR2 stimulation (blue); male context (green) and pup (orange). Warmer colours indicate higher similarity, which is quantified in **a**. These data show that the repertoire of USV syllables evoked by photostimulation are rich and varied. When compared to natural USVs, they are similar to those produced by wild-type male mice as they interact with live female mice; and less similar to USVs evoked by male cues and pup USVs.

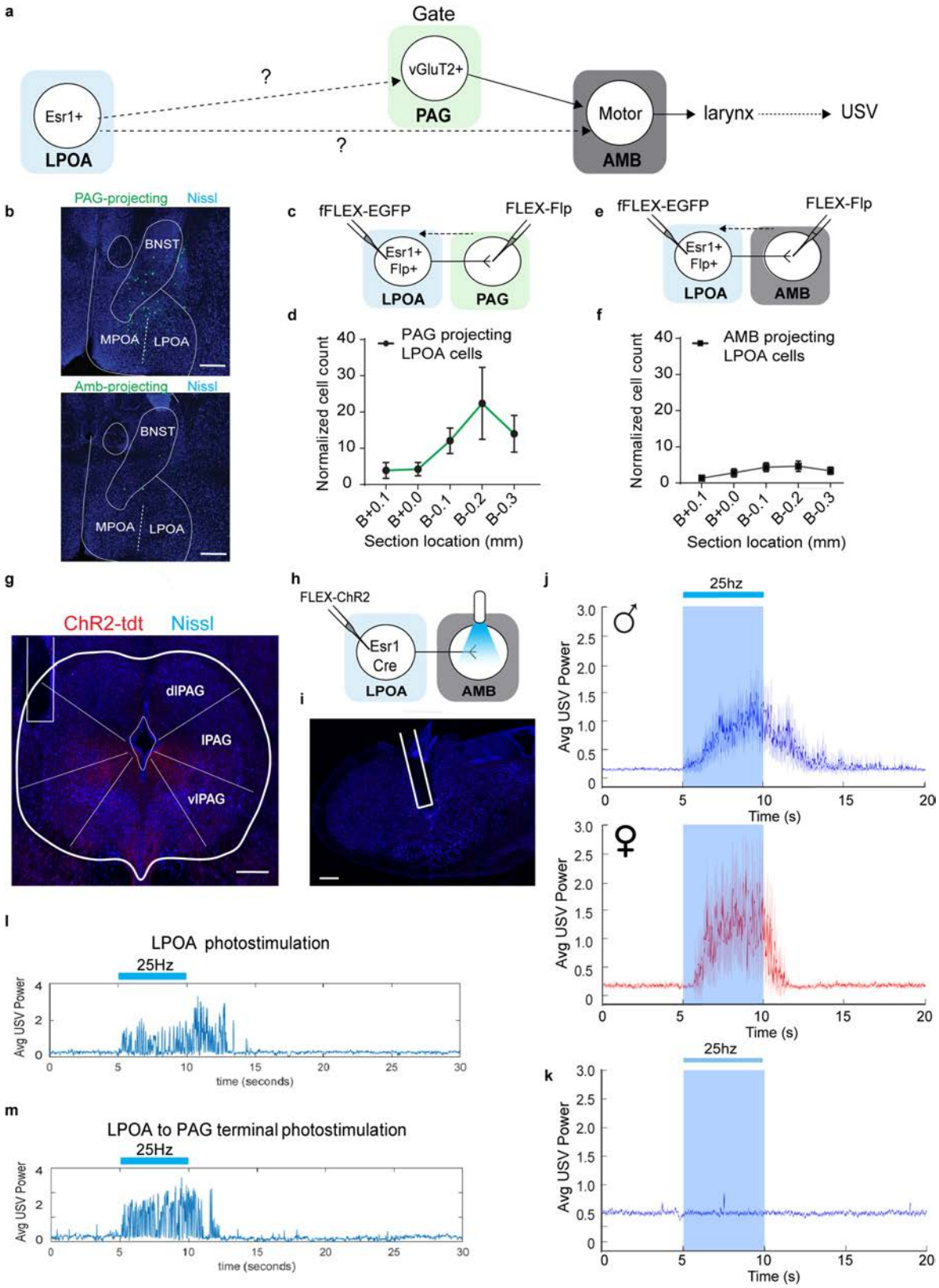

Extended Data Fig. 5 | See next page for caption.

Extended Data Fig. 5 | LPOA^{ESR1} projections to USV motor centre (ambiguous) are sparse and unable to be functionally validated, whereas LPOA^{ESR1} projections to PAG produces robust USV production. a, Strategy to test whether LPOA^{ESR1} neurons are anatomically or functionally connected to either the PAG or the nucleus ambiguous, which are known to evoke USV calling in the mouse[16,17,50,51]. **b**–**f**, Retrograde tracing experiment from either PAG or nucleus ambiguous to label LPOA^{ESR1} cell projections by injecting a Cre-dependent FLP-expressing pseudotyped equine infectious anaemia virus (RG-EIAV-FLEX-Flp) in either the PAG or nucleus ambiguous, and a FLP-dependent AAV expressing eGFP in the LPOA of ESR1-Cre mice[32,33]. We confirmed the specificity of viral expression by multiplex fluorescent in situ hybridization (Extended Data Fig. 6a, b). We observed sparse labelling of LPOA cells that directly project to the nucleus ambiguous, and a larger population centred in the LPOA region (previously showed to be co-labelled by c-FOS and ESR1) that directly project to the region of the PAG USV-gate neurons. **b**, Example image of PAG-projecting (top) or nucleus ambiguous-projecting (bottom) eGFP$^+$ cells in the LPOA as described and quantified in **c**–**f**. Scale bar, 200 µm. $n = 5$ mice; 5 sections per mouse. **c**, **d**, Anatomical tracing from the PAG to the LPOA resulted in robust labelling. **c**, Experimental design to express the FLEX-FLP virus in the PAG and fFLEX-eGFP in the LPOA of ESR1-Cre mice. **d**, Restrocaudal distribution of the total number of PAG-projecting eGFP$^+$ cells in the LPOA. Data are mean ± s.e.m. $n = 5$ mice. **e**, **f**, Anatomical tracing from the nucleus ambiguous to the LPOA resulted in sparse labelling. **e**, Experimental design to express FLEX-FLP virus in the nucleus ambiguous and fFLEX-eGFP in the LPOA of ESR1-Cre mice. **f**, Restrocaudal distribution of the total number of nucleus ambiguous-projecting eGFP$^+$ cells in the LPOA. Data are mean ± s.e.m. $n = 5$ mice. To test whether either of these projections function to evoke USV calling, we expressed ChR2 in the LPOA of ESR1-Cre mice and photostimulated from axon terminals in either the PAG or the nucleus ambiguous. **g**, Sample image of optical fibre position for stimulation of LPOA$^{ESR1/ChR2}$ terminals in the PAG show in **j**. **h**, Experimental design for stimulation of LPOA$^{ESR1/ChR2}$ terminals in the nucleus ambiguous. **i**, Sample image of optical fibre position for terminal stimulation in the nucleus ambiguous. Scale bar, 200 µm. $n = 5$ mice, 4 sections per mouse. **j**, Average USV power across the 40–90-kHz band of recording during PAG terminal stimulation. Solid line indicates the mean and shaded region indicate 95% confident interval (blue shading, $n = 13$ male mice; red shading, $n = 4$ female mice; 4 trials per mouse). **k**, Average USV power across 40–90-kHz band of recording during terminal stimulation of the nucleus ambiguous. Solid line indicates the mean and shaded region indicate 95% confident interval (blue shading, $n = 5$ male mice, 4 trials per mouse). **l**, **m**, Average USV power during single trials of the same male stimulated with 25 Hz for 5 s from either LPOA$^{ESR1/ChR2}$ cell somas (**l**) or LPOA$^{ESR1/ChR2}$ axon terminals in the PAG (**m**).

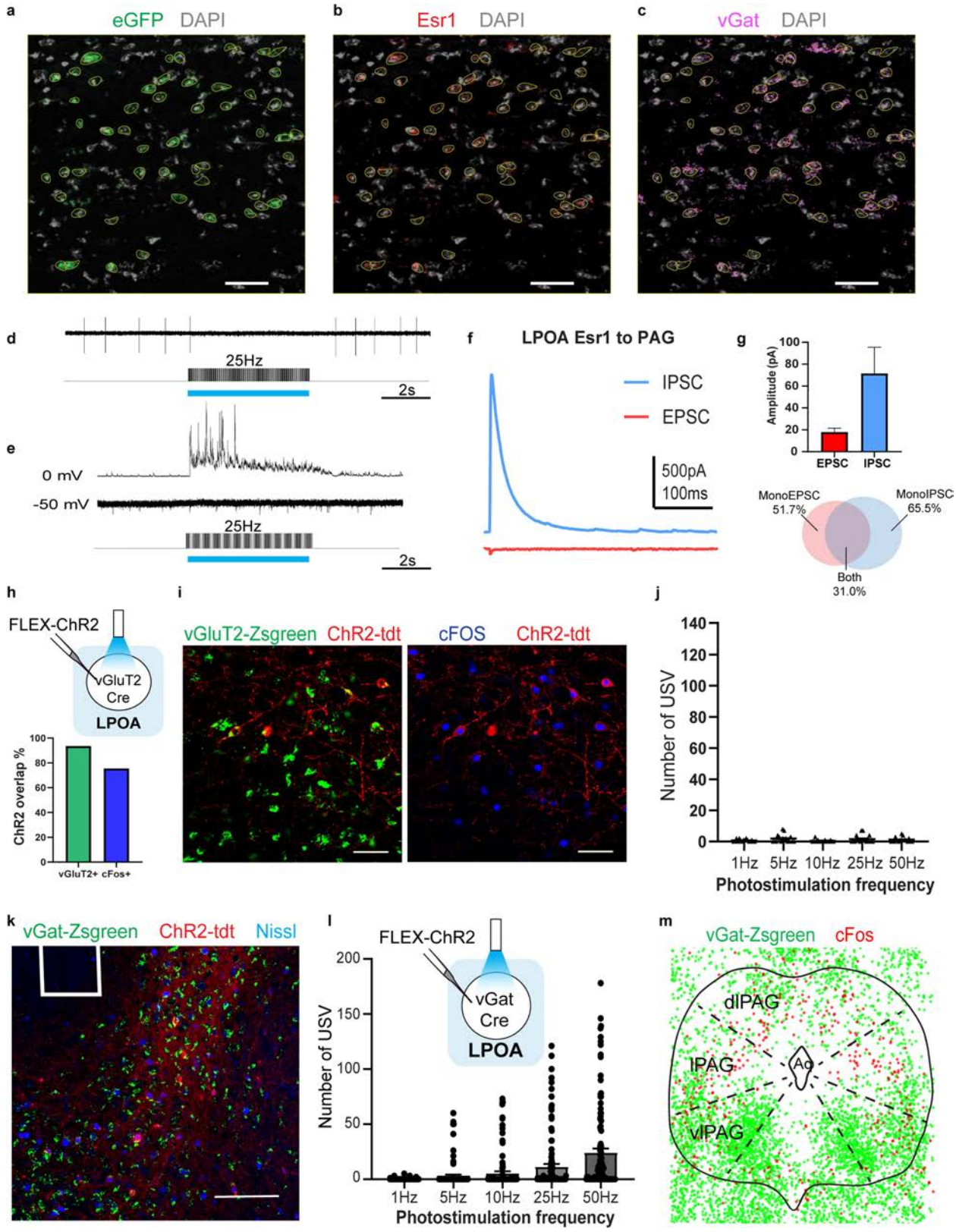

Extended Data Fig. 6 | See next page for caption.

Extended Data Fig. 6 | LPOA-PAG projecting cells are largely inhibitory and stimulation of LPOA^{VGAT} cells elicits USVs. a–**c**, RNAScope multiplex in situ hybridization histology of LPOA sections after injection of retro travelling Cre-dependent FLP-expressing virus in the PAG and a FLP-dependent eGFP (AAV-fFLEX-dGFP) in the LPOA of ESR1-Cre mice (see Extended Data Fig. 4c, d) reveals overlap of eGFP (green) (**a**), ESR1 (red) (**b**) and VGAT (magenta) (**c**) probes. Yellow traces are eGFP^{+} cells used as regions of interest and applied to ESR1 and VGAT channels for analysis. Scale bar, 50 µm. $n = 3$ mice, >3 sections per mouse with RNAScope staining. **d**–**g**, Electrophysiology recording of PAG neurons in ex vivo slice shows functional inhibition. **d**, Sample trace showing cell-attached recording of a PAG cell. **e**, IPSC and EPSC recordings while photostimulating (blue bars) LPOA$^{ESR1/ChR2}$ terminals. **f**, IPSC and EPSC recordings during single light pulse. **g**, Peak conductance (calculated by amplitude or driving force) of EPSC (red) and IPSC (blue) recordings. Data are mean ± s.e.m. Bottom, percentage of observed cells with monosynaptic IPSCs (blue), EPSCs (red), or both (grey). $n = 5$ mice, 29 cells. **h**, **i**, Strategy to test whether LPOA excitatory neurons elicit USVs. **h**, Top, experimental design to express ChR2 in the LPOA of VGLUT2-Cre knock-in mice. Bottom, percentage of ChR2 overlap with either the VGLUT2-ZsGreen marker or c-FOS staining. **i**, Sample images showing overlap between ChR2 with VGLUT2-ZsGreen or c-FOS staining. Scale bars, 50 µm. $n = 4$ mice, 7 images per mouse used for cell quantification. **j**, Number of USVs emitted during light stimulation of LPOA$^{VGLUT2/ChR2}$ neurons. $n = 4$, 16 trials per condition. **k**, Sample image indicating fibre position (white square) and ChR2 expression in the LPOA of VGAT-ZsGreen mice. Scale bars, 200 µm. $n = 9$ mice, 4 sections per mouse collected. **l**, Experimental design to express ChR2 in LPOA of VGAT-Cre mice and the number of USV syllables emitted during light stimulation of LPOA$^{VGAT/ChR2}$ neurons. Data are mean ± s.e.m. $n = 9$ mice, 91 trials per condition. **m**, Composition of c-FOS expression (after odour-evoked USVs) in the PAG of VGAT-Cre mice. c-FOS^{+} cells (red) are largely VGAT^{-} (consistent with PAG USV gate neurons being excitatory), whereas VGAT neurons are largely clustered in the ventrolateral PAG[52]. $n = 3$ mice, overlay of 100-µm thick sections roughly at bregma −4.4 mm.

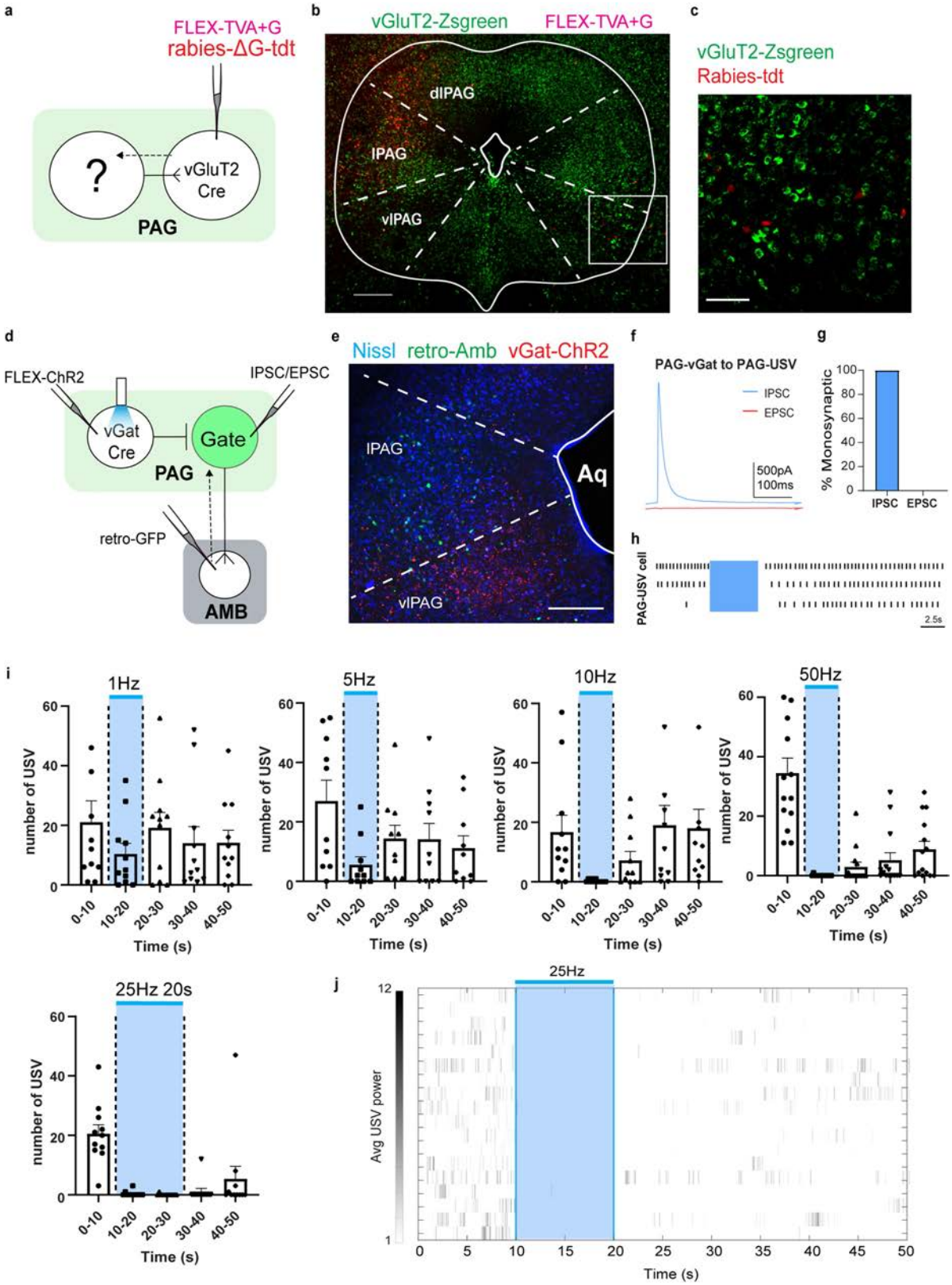

Extended Data Fig. 7 | See next page for caption.

Extended Data Fig. 7 | Local PAG^{VGAT} neurons inhibit PAG USV-gate cells, and photostimulation inhibits natural USVs. Most immediate neurons 'upstream' of the PAG USV-gate cells are VGLUT2$^-$ neurons in the PAG, ipsilateral to the PAG^{VGLUT2} neurons. **a**, Experimental design for rabies viral tracing from the PAG of VGLUT2-Cre knock-in mice. **b**, Sample PAG image from rabies tracing. Red cells on the left are cells infected with the TVA+G helper virus that overlaps with VGLUT2-ZsGreen (starter cells). The white box on the right is enlarged and showed in **c**. Scale bars, 250 µm. **c**, In total, 76 out of 87 cells labelled with rabies-tdTomato (87%) observed in ventrolateral PAG do not overlap with VGLUT2-ZsGreen cells, which suggests that they probably express VGAT. Scale bar, 100 µm. $n = 5$ mice, total 32 sections counted. To functionally test whether the PAG USV-gate neurons are subjected to local inhibition, we engineered male mice to express ChR2 in the local PAG inhibitory cells (PAG$^{VGAT/ChR2}$) and injected retroAAV-eGFP in the nucleus ambiguous to specifically identify PAG USV-gate neurons. **d**, Experimental design for retrograde labelling from the nucleus ambiguous to PAG USV-gate neurons, and optical manipulation of PAG$^{VGAT/ChR2}$ cells for behaviour and physiology. **e**, Sample image of PAG section showing nucleus ambiguous-projecting cells in lateral PAG (green) and VGAT/ChR2-expressing cells (red) in ventrolateral PAG. Scale bar, 100 µm. Aq, aqueduct, fourth ventricle. Ex vivo whole-cell recordings and cell-attached recordings showed that all tested PAG^{GFP} neurons (USV-gating neurons) were inhibited within 5 ms after photostimulation of PAG$^{VGAT/ChR2}$ neurons, consistent with monosynaptic inhibitory inputs. $n = 2$ mice, 2 sections per mouse collected. **f**–**h**, Ex vivo slice electrophysiology recordings of PAG USV-gate cells while photostimulating PAG$^{VGAT/ChR2}$ neurons. **f**, IPSC and EPSC recordings during a single light pulse. **g**, Photostimulation of PAG$^{VGAT/ChR2}$ neurons generate monosynaptic iPSCs in all cells investigated. $n = 2$ mice, 14 cells recorded. **h**, Cell-attached physiology of USV-gate neurons (PAG^{GFP}). Blue shading indicates photostimulation period. Each line showed as individual cell recorded. **i**, **j**, Stimulating local PAG^{VGAT} neurons inhibit socially evoked USVs. **i**, Increasing the frequency or duration of photostimulation (5 s of 1 Hz, 5 Hz, 10 Hz, 50 Hz and 10 s of 25 Hz) of PAG$^{VGAT/ChR2}$ neurons from male mice during interaction with awake behaving female mice to evoke natural USVs. Blue bar/shading denotes light stimulation. Number of USVs are calculated in 10-s time bins. Data are mean ± s.e.m. $n = 3$ mice, 5–6 trials per mouse per condition. **j**, Raster plot of USVs emitted before, during and after photostimulation at 25 Hz for 5 s, as showed in Fig. 2e. Blue light indicates light stimulation period. Each row is a single trial. Data are mean ± s.e.m. $n = 3$ mice, 19 trials.

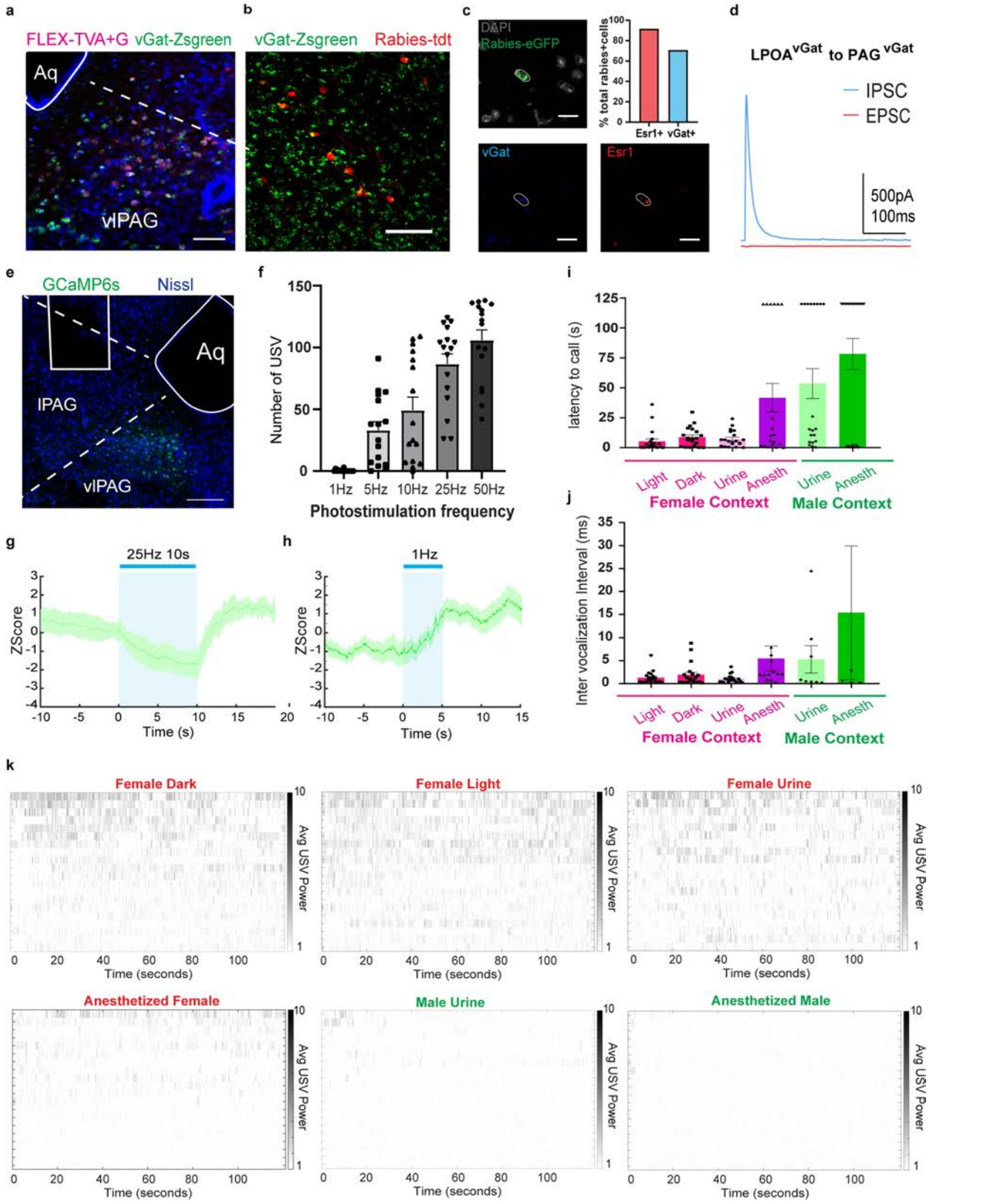

Extended Data Fig. 8 | See next page for caption.

Extended Data Fig. 8 | LPOA^{VGAT} cell population connect to PAG^{VGAT} cell population both anatomically and functionally, and the number of USV syllables and latency flexibly varies with social context. **a**, Example image of PAG section for experiment described in Fig. 2f, g. Starter cells (magenta) overlap with VGAT-ZsGreen. Scale bar, 100 µm. **b**, Sample image of LPOA section for experiment described in Fig. 2f, g showing overlap of rabies-tdTomato^{+} cells (red) with VGAT-ZsGreen (272 out of 320 cells counted, $n = 3$ mice, total of 17 sections). Scale bar, 200 µm. **c**, Example image of RNAScope multiplex in situ hybridization in LPOA to complement Fig. 2f. Sections are stained with eGFP (green), VGAT (blue) and ESR1(red) probes. Scale bars, 25 µm. Most LPOA neurons that projected to PAG^{VGAT} neurons co-express ESR1. $n = 2$ mice, 16 sections (20-µm thick) collected. Top right, quantification of rabies-positive cells overlapping with VGAT^{+} or ESR1^{+} using RNAScope multiplex in situ hybridization ($n = 2$ mice, total 24 rabies-positive cells quantified. **d**, PAG^{VGAT} cells receive monosynaptic IPSC from LPOA$^{VGAT/ChR2}$ neurons. IPSCs and EPSCs evoked by single light pulse ($n = 5$ mice, 16 cells recorded). **e**–**h**, To study the in vivo effects of LPOA^{ESR1} neuron activity, we expressed ChR2 in the LPOA and GCaMP6s in the PAG of VGAT-Cre mice (LPOA$^{VGAT/ChR2}$;PAG$^{VGAT/GCaMP6s}$). Photostimulation in the LPOA of awake behaving mice resulted in a decrease in fibre photometry as measured GCaMP6s fluorescence in the local PAG inhibitory neurons and an accompanying initiation of USV production. **e**, Representative image of fibre track and viral expression of GCaMP6s in the PAG. Scale bar, 200 µm. $n = 4$ mice, 3 sections per mouse. **f**, Number of USV syllables emitted following light stimulation of LPOA$^{VGAT/ChR2}$ neurons while recording of PAG$^{VGAT/GCaMP6s}$ signals. Data are mean ± s.e.m. $n = 4$, 16 trials per condition. **g**, Mean z-score of fibre photometry signal from PAG$^{VGAT/GCaMPs}$ with photostimulation at 25 Hz for 10 s of LPOA$^{VGAT/ChR2}$ cells. **h**, Mean z-score of fibre photometry signal from PAG$^{VGAT/GCaMPs}$ neurons with photostimulation at 1 Hz for 5 s of LPOA$^{VGAT/ChR2}$ cells, in which the photostimulation is below the threshold to produce USVs. Solid line indicates mean of signals and shaded region indicates 95% confident intervals. $n = 4$ mice, 3 trials per mouse. **i**–**k**, To study the extent of USV syllable flexibility during natural social behaviour, we collected USVs from wild-type male mice during different social contexts. Wild-type male mouse USVs were recorded during 2-min interactions with a variety of socially relevant sensory contexts including the presence of an awake female mouse (in the dark or light), female urine, an anaesthetized female mouse, male urine, or an anaesthetized male mouse. The flexibility of social vocalization is underscored by the longer and louder USV bouts triggered by awake behaving female mice compared to the USVs evoked by anaesthetized female mice even though much of the contextual sensory cues are similar. **i**, Latency to first USV evoked by different sensory contexts. **j**, Average inter vocalization intervals of USVs evoked by different sensory stimuli. Red bar denotes female context (live female mouse in either the dark with red light or bright light, female urine, anaesthetized female mouse); green bar denotes the male context (male urine or anaesthetized male mouse). Data are mean ± s.e.m. $n = 20$ mice. **k**, Raster plot of USVs emitted while interacting with different sensory contexts. Each line is a single wild-type male. Average USV power is calculated by mean decibels in the 40–90-kHz band from raw recording.

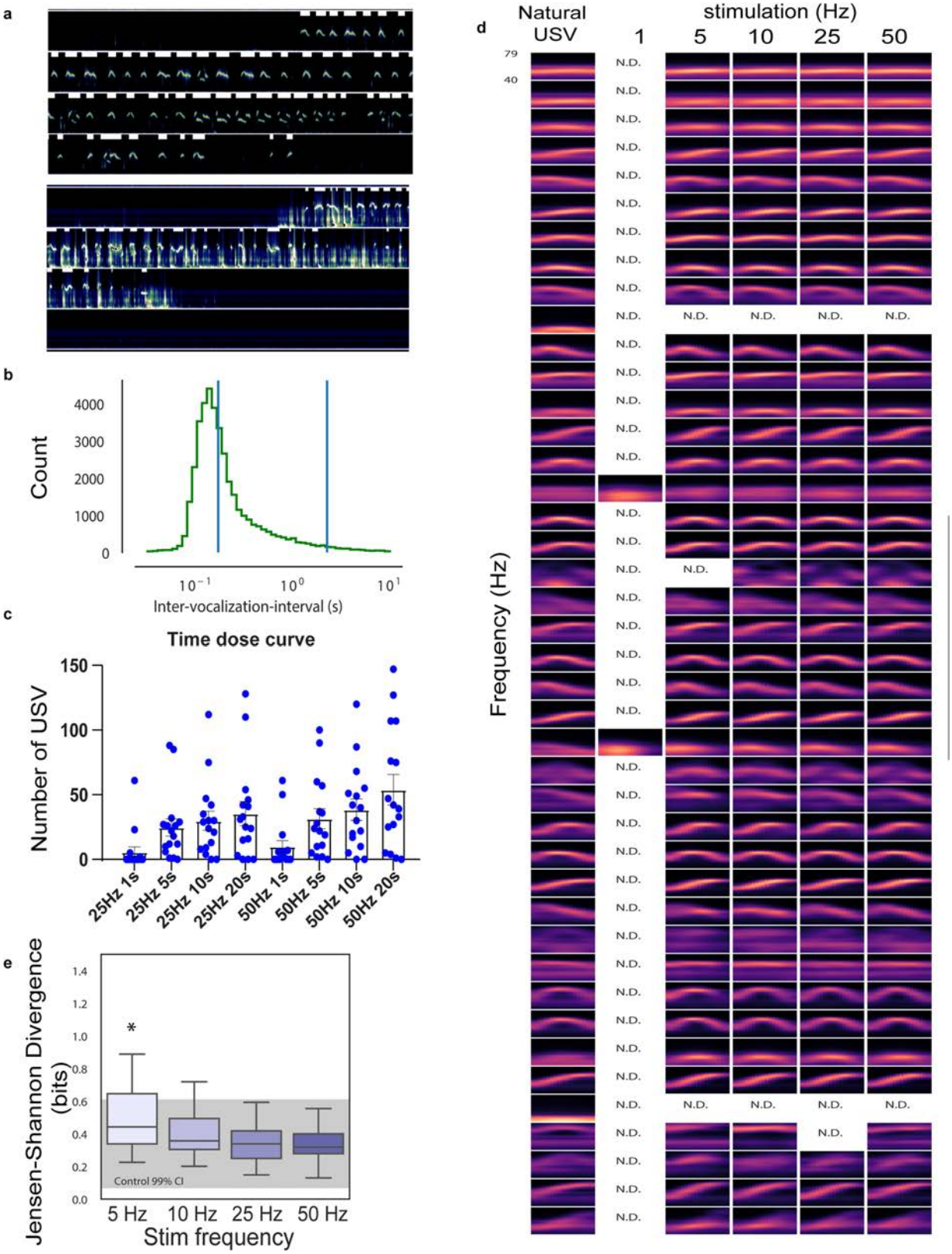

Extended Data Fig. 9 | See next page for caption.

Extended Data Fig. 9 | Increasing LPOA^{ESR1} neuron activity generates more USV syllables without altering syllable identity. a, Two sonograms (12-s long each) analysed for USV production. White bars (top of each 3-s line) indicate the production and duration of USV syllables automatically identified. In the top sonogram, there was little additional acoustic noise so USV syllables are easy to identify; in the bottom sonogram, although there is abundant low-frequency noise (from self-movement or from interactions with another individual during the USV recording), the white bars robustly identify USV syllables. **b**, To determine whether USV bout length is fixed or variable, we analysed the inter-USV vocalization intervals, and found a natural threshold of 2-s pauses as a basis to define the end of a USV bout[23]. **c**, Number of USVs emitted after photostimulation of LPOA$^{ESR1/ChR2}$ cells at 25 Hz or 50 Hz and 1–20-s duration. Data are mean ± s.e.m. $n = 16$ mice. **d**, Syllables maintain their identity and structure from 1–50-Hz photostimulation of LPOA$^{ESR1/ChR2}$ neurons. **e**, Jensen–Shannon divergence score of USVs produced by 1–50-Hz photostimulation of LPOA$^{ESR1/ChR2}$ cells compared to natural USVs during interaction with female urine or live female mice. Box plot denotes the minimum and maximum values and quantile (0.25, 0.75). Grey shading denotes the 95% confident interval of the control data. To compute *P* values, we randomly choose mice with no stimulation and mice with ChR2 stimulation and computed the Jensen–Shannon divergence score. This step was repeated 1,000 times to build a null distribution. We then computed the probability that each bootstrap exceeded the observed median at each stimulation frequency. We found that a stimulation frequency of only 5 Hz resulted in a significant *P* value. $^{*}P = 0.036$, $n = 26$ mice.

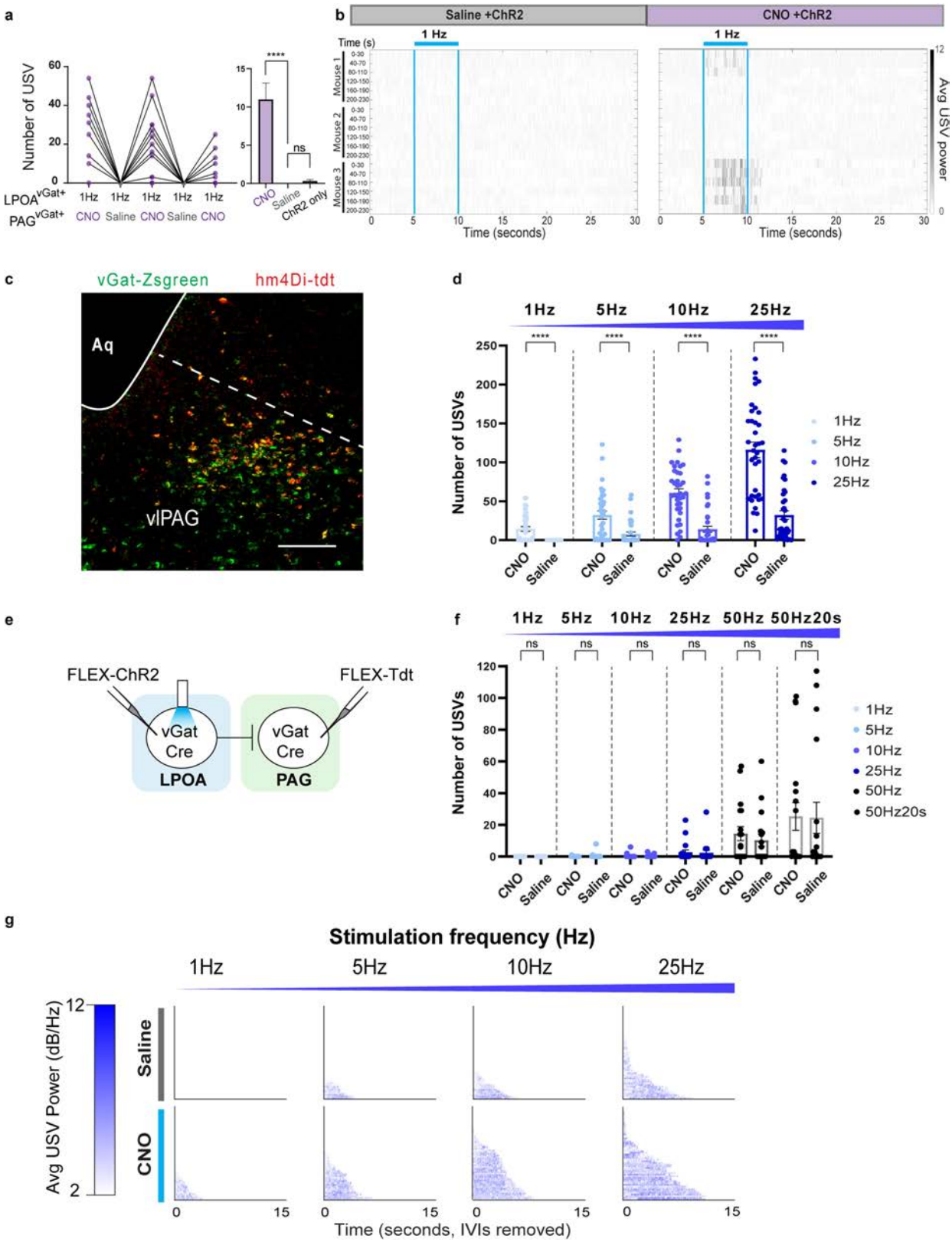

Extended Data Fig. 10 | See next page for caption.

Extended Data Fig. 10 | Circuit and intrinsic properties of PAG^{VGAT} neurons support USV persistence. a, **b**, USVs emitted during photostimulation of LPOA$^{VGAT/ChR2}$ cells with injection of saline as control (grey) or CNO (purple) to inhibit PAG$^{VGAT/hM4Di}$ neurons on alternative days. **a**, Number of USVs emitted with 1 Hz 5s light stimulation. **b**, Raster plot of USVs emitted during and after photostimulation (blue bars). Each row is 30 s of a 230-s trial aligned to light stimuli applied every 40 s. Data are mean ± s.e.m. $n = 3$, 6 trials per mouse per test day. ****$P < 0.0001$, paired Wilcoxon test, two sided. ns, not significant ($P > 0.05$). **c**, Representative image of co-expression of hM4Di-tdTomato with VGAT-ZsGreen cells in the PAG. Scale bar, 200 µm. $n = 2$ mice, 2 sections per mouse collected. **d**, Number of USVs emitted during increased frequency photostimulation in LPOA of male mice expressing LPOA$^{VGAT/ChR2}$ and PAG$^{VGAT/hM4Di}$ and injected with CNO or saline on alternative days. $n = 3$, 36 trials per condition. Data are mean ± s.e.m. ****$P < 0.0001$, Wilcoxon test, two sided. **e**, Experimental design to express control virus (tdTomato) in the PAG of VGAT-Cre mice (Fig. 4e, f). **f**, Number of USVs emitted by photostimulating LPOA^{VGAT} cells under either CNO or saline conditions in mice expressing FLEX-tdTomato viral control (PAG$^{VGAT/tdTomato}$) (control). $n = 3$, 18 trials per condition. Data are mean ± s.e.m. ns, not significant ($P > 0.05$), Wilcoxon test, two sided. **g**, Raster plot of USV bouts emitted during either CNO or saline test days under different stimulation frequency. Note that *Drosophila* courtship songs show similar feature separation across the circuit with songs evoked by pIP10 neurons tightly locked to stimulation (like the PAG USV-gate neurons) compared to calling generated by P1 neurons that persists beyond stimulation (as with the LPOA^{ESR1} neurons)[53]. This suggests diverse social species use general circuit strategies to maintain persistent auditory responses that outlast the detection of sensory information.

nature research

Corresponding author(s): Lisa Stowers

Last updated by author(s): 3/1/2021

Reporting Summary

Nature Research wishes to improve the reproducibility of the work that we publish. This form provides structure for consistency and transparency in reporting. For further information on Nature Research policies, see our Editorial Policies and the Editorial Policy Checklist.

Statistics

For all statistical analyses, confirm that the following items are present in the figure legend, table legend, main text, or Methods section.

n/a	Confirmed
☐	☒ The exact sample size (*n*) for each experimental group/condition, given as a discrete number and unit of measurement
☐	☒ A statement on whether measurements were taken from distinct samples or whether the same sample was measured repeatedly
☐	☒ The statistical test(s) used AND whether they are one- or two-sided *Only common tests should be described solely by name; describe more complex techniques in the Methods section.*
☒	☐ A description of all covariates tested
☐	☒ A description of any assumptions or corrections, such as tests of normality and adjustment for multiple comparisons
☐	☒ A full description of the statistical parameters including central tendency (e.g. means) or other basic estimates (e.g. regression coefficient) AND variation (e.g. standard deviation) or associated estimates of uncertainty (e.g. confidence intervals)
☐	☒ For null hypothesis testing, the test statistic (e.g. *F*, *t*, *r*) with confidence intervals, effect sizes, degrees of freedom and *P* value noted *Give P values as exact values whenever suitable.*
☒	☐ For Bayesian analysis, information on the choice of priors and Markov chain Monte Carlo settings
☒	☐ For hierarchical and complex designs, identification of the appropriate level for tests and full reporting of outcomes
☒	☐ Estimates of effect sizes (e.g. Cohen's *d*, Pearson's *r*), indicating how they were calculated

Our web collection on statistics for biologists contains articles on many of the points above.

Software and code

Policy information about availability of computer code

Data collection	Matlab R2019b (Fiber Photometry data collection); SeaWave 2.0 (USV recording); Nikon-Elements (Confocal imaging); pClamp10 software (slice recording)
Data analysis	Matlab R2019b (USV analysis, MUPET), Python version 3.6 and beyond (syllable classification); Nikon-Elements (cell counting); Graphpad Prism 8.30

For manuscripts utilizing custom algorithms or software that are central to the research but not yet described in published literature, software must be made available to editors and reviewers. We strongly encourage code deposition in a community repository (e.g. GitHub). See the Nature Research guidelines for submitting code & software for further information.

Data

Policy information about availability of data

All manuscripts must include a data availability statement. This statement should provide the following information, where applicable:

- Accession codes, unique identifiers, or web links for publicly available datasets
- A list of figures that have associated raw data
- A description of any restrictions on data availability

The data in this study is available from the corresponding author upon request.

Field-specific reporting

Please select the one below that is the best fit for your research. If you are not sure, read the appropriate sections before making your selection.

☒ Life sciences ☐ Behavioural & social sciences ☐ Ecological, evolutionary & environmental sciences

For a reference copy of the document with all sections, see nature.com/documents/nr-reporting-summary-flat.pdf

Life sciences study design

All studies must disclose on these points even when the disclosure is negative.

Sample size	Sample sizes were determined based on previous studies. (See Tschida,K et.al, Neruon 2019 and Chabout, J., et.al, J Vis Exp, 2017)
Data exclusions	Detailed in the Methods "ChR2 stimulation" and "Fiber Photometry" sections. The exclusion for ChR2 stimulation data is pre-established, however, the exclusion for Fiber photometry experiment was established based on observation during the experiment.
Replication	For ChR2 stimulation as well as Fiber photometry, all stimulation/recordings were repeated at least for 4 times across multiple test days. We also have repeated LPOA photostimulation and recordings in several batches of animals to confirm our findings.
Randomization	The surgery for all functional test are done prior to behavior test so no randomization was used. The stimulus given to wildtype mice (data showed in fig 3) are collected in a random order.
Blinding	Cell count was performed by a blinded party where the purpose of the experiment was not explained until the quantification was done. All functional manipulation or imaging experiment were not performed blinded because they all performed by the same individual.

Reporting for specific materials, systems and methods

We require information from authors about some types of materials, experimental systems and methods used in many studies. Here, indicate whether each material, system or method listed is relevant to your study. If you are not sure if a list item applies to your research, read the appropriate section before selecting a response.

Materials & experimental systems

n/a	Involved in the study
☐	☒ Antibodies
☒	☐ Eukaryotic cell lines
☒	☐ Palaeontology and archaeology
☐	☒ Animals and other organisms
☒	☐ Human research participants
☒	☐ Clinical data
☒	☐ Dual use research of concern

Methods

n/a	Involved in the study
☒	☐ ChIP-seq
☒	☐ Flow cytometry
☒	☐ MRI-based neuroimaging

Antibodies

Antibodies used	Anti-ESR1 antibody (Millipore, Estrogen Receptor Alpha, Rabbit, 06935MI) Secondary antibody (ThermoFisher Alexa-Fluor 488 or 647 anti-rabbit IgG H+L)
Validation	Anti-ESR1 antibody (manufacture validated in Murine species) Secondary antibody (validated by manufacture)

Animals and other organisms

Policy information about studies involving animals; ARRIVE guidelines recommended for reporting animal research

Laboratory animals	BALB/cByJ male mice were group housed at weaning, single housed at 8 weeks old for at least one week before any testing and maintained on a 12/12hr light/dark cycle with food and water available ad libitum in a controlled environment (median temperature 70 degree, humidity 50%). For functional manipulation, females and males from mouse lines are purchased from The Jackson Laboratory: Esr1-Cre (stock #: 017911), vGat-Cre (stock #: 016962), vGluT2-Cre (stock #: 016963), and ROSA-LSL-ZsGreen (Ai6, stock #: 007906). All mice were backcrossed into the BALB/cByJ background for >5 generations except for the ROSA-LSL-Zsgreen line. Surgeries were performed between 2-6 months old and animals were given 2-3 weeks for recovery before behavioral testing that last for 2-5 weeks.
Wild animals	*Provide details on animals observed in or captured in the field; report species, sex and age where possible. Describe how animals were caught and transported and what happened to captive animals after the study (if killed, explain why and describe method; if released,*

	say where and when) OR state that the study did not involve wild animals.
Field-collected samples	*For laboratory work with field-collected samples, describe all relevant parameters such as housing, maintenance, temperature, photoperiod and end-of-experiment protocol OR state that the study did not involve samples collected from the field.*
Ethics oversight	All animal procedures were conducted in accordance with institutional guidelines and protocols approved by the Institutional Animal Care and Use Committee at Scripps Research.

Note that full information on the approval of the study protocol must also be provided in the manuscript.